Robotics: Advanced Concepts & Analysis

Module 10 - Advanced Topics

Ashitava Ghosal[1]

[1]Department of Mechanical Engineering
&
Centre for Product Design and Manufacture
Indian Institute of Science
Bangalore 560 012, India
Email: asitava@mecheng.iisc.ernet.in

NPTEL, 2010

OUTLINE

Contents of Lecture[1]

- Introduction to non-linear dynamics and chaos.
- Chaos in robot control equations.
- Simulation results
- Analytical criteria
- Summary

[1] Major portions of this Lecture are from Shrinivas & Ghosal (1996 & 1997) and Ravishankar & Ghosal (1999). More details are available in these and other references listed at the end of the module.

CONTENTS OF LECTURE[1]

- Introduction to non-linear dynamics and chaos.
- Chaos in robot control equations.
- Simulation results
- Analytical criteria
- Summary

[1]Major portions of this Lecture are from Shrinivas & Ghosal (1996 & 1997) and Ravishankar & Ghosal (1999). More details are available in these and other references listed at the end of the module.

Contents of Lecture[1]

- Introduction to non-linear dynamics and chaos.
- Chaos in robot control equations.
- Simulation results
- Analytical criteria
- Summary

[1] Major portions of this Lecture are from Shrinivas & Ghosal (1996 & 1997) and Ravishankar & Ghosal (1999). More details are available in these and other references listed at the end of the module.

CONTENTS OF LECTURE[1]

- Introduction to non-linear dynamics and chaos.
- Chaos in robot control equations.
- Simulation results
- Analytical criteria
- Summary

[1] Major portions of this Lecture are from Shrinivas & Ghosal (1996 & 1997) and Ravishankar & Ghosal (1999). More details are available in these and other references listed at the end of the module.

CONTENTS OF LECTURE[1]

- Introduction to non-linear dynamics and chaos.
- Chaos in robot control equations.
- Simulation results
- Analytical criteria
- Summary

[1] Major portions of this Lecture are from Shrinivas & Ghosal (1996 & 1997) and Ravishankar & Ghosal (1999). More details are available in these and other references listed at the end of the module.

Introduction

Chaotic Systems

- *Deterministic* physical and mathematical systems whose time history has *sensitive dependence on initial conditions*.
- Occurs in *many non-linear* dynamical systems[2].
  - Observed in a wide range of systems such as in electric circuits, fluid dynamics, double pendulum (Levien and Tan (1993)), large deformation in plates, mechanical and electro-mechanical systems with friction and hysteresis(Sekar and Narayanan (1992)), and several mathematical equations modeling complex phenomenon such as weather.
  - Controversially related to fields such as economics and medical phenomenon such as epilepsy.
  - Origin: classical gravitational 3– body problem (Poincaré late 19th century).
- Duffing's equation (see Moon (1987) & Dowell and Pezeshki (1986)) is a common and well-studied example
  - $\ddot{X} + C\dot{X} + X^3 = B\cos\ t$
  - Spring-mass-damper system with non-linear 'hardening' spring.
  - Different time histories for different values of C and B.

[2] See link for more details.

Introduction

Chaotic Systems

- *Deterministic* physical and mathematical systems whose time history has *sensitive dependence on initial conditions*.
- Occurs in *many non-linear* dynamical systems[2].
  - Observed in a wide range of systems such as in electric circuits, fluid dynamics, double pendulum (Levien and Tan (1993)), large deformation in plates, mechanical and electro-mechanical systems with friction and hysteresis(Sekar and Narayanan (1992)), and several mathematical equations modeling complex phenomenon such as weather.
  - Controversially related to fields such as economics and medical phenomenon such as epilepsy.
  - Origin: classical gravitational $3-$ body problem (Poincaré late 19th century).
- Duffing's equation (see Moon (1987) & Dowell and Pezeshki (1986)) is a common and well-studied example
  - $\ddot{X} + C\dot{X} + X^3 = B\cos\ t$
  - Spring-mass-damper system with non-linear 'hardening' spring.
  - Different time histories for different values of C and B.

[2]See link for more details.

INTRODUCTION

CHAOTIC SYSTEMS

- *Deterministic* physical and mathematical systems whose time history has *sensitive dependence on initial conditions*.
- Occurs in *many non-linear* dynamical systems[2].
  - Observed in a wide range of systems such as in electric circuits, fluid dynamics, double pendulum (Levien and Tan (1993)), large deformation in plates, mechanical and electro-mechanical systems with friction and hysteresis(Sekar and Narayanan (1992)), and several mathematical equations modeling complex phenomenon such as weather.
  - Controversially related to fields such as economics and medical phenomenon such as epilepsy.
  - Origin: classical gravitational 3− body problem (Poincaré late 19th century).
- Duffing's equation (see Moon (1987) & Dowell and Pezeshki (1986)) is a common and well-studied example
  - $\ddot{X} + C\dot{X} + X^3 = B\cos\ t$
  - Spring-mass-damper system with non-linear 'hardening' spring.
  - Different time histories for different values of C and B.

[2] See link for more details.

Introduction

Chaotic Systems

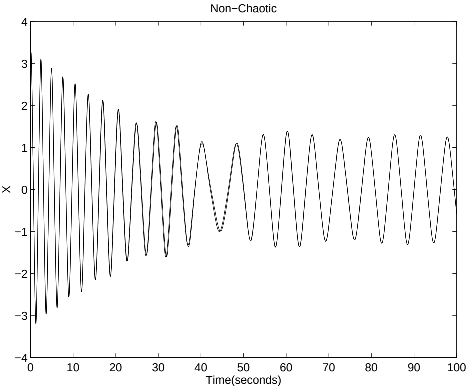

Figure 1: Non-chaotic behaviour of a Duffing's oscillator

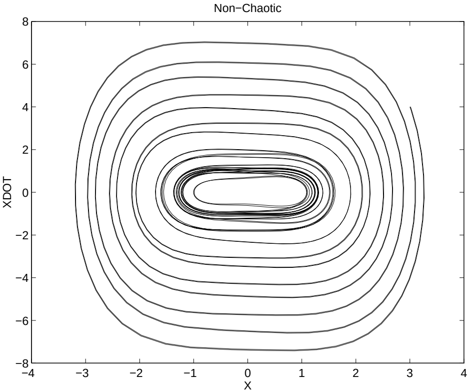

Figure 2: Phase plot – $\dot{X}(t)$ Vs. $X(t)$ – in non-chaotic case

- $C = 0.08$ $B = 0.2$, Initial Conditions — $(3.0, 4.0)$ and $(3.01, 4.01)$
- Two trajectories do not deviate much as time increases and phase plot settle to a limit cycle!

INTRODUCTION

CHAOTIC SYSTEMS

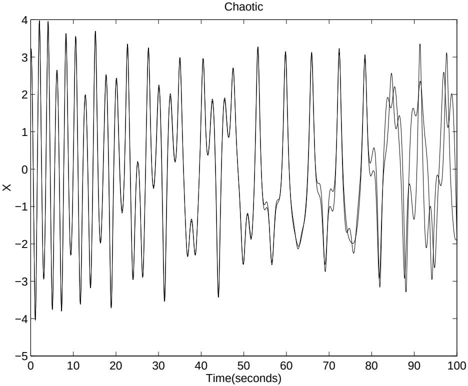

Figure 3: Chaotic behaviour of a Duffing's oscillator

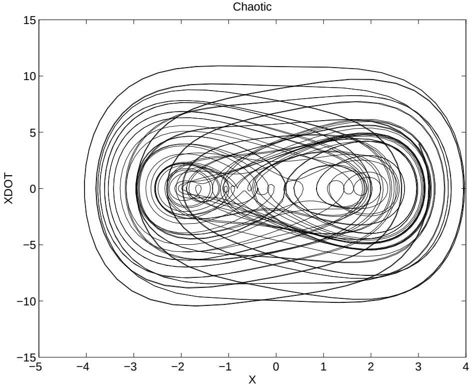

Figure 4: Phase plot – $\dot{X}(t)$ Vs. $X(t)$ – in chaotic case

- $C = 0.05$ $B = 7.5$, Initial Conditions — $(3.0, 4.0)$ and $(3.01, 4.01)$
- Large deviation in two trajectories as t increases and *dense* phase plot.

Introduction

Key Features of Chaotic Systems

- Main features of a chaotic system:
  - Sensitive dependence on initial conditions (see Duffing's equation) for certain parameter values.
  - Every point in phase space is *eventually visited* – Periodic system (single or finitely many periods), phase plot will *settle* in a region (see limit cycle in Duffing's equation).
  - Chaotic system, the *attractor* is *not* a *fixed point* or a *limit cycle* $\rightarrow$ *Strange attractor* has *fractal* dimension!
- Only in *non-linear* dynamical systems – Finite dimensional linear systems *can never* exhibit chaos.
- In *continuous* non-linear dynamical system (described by differential equation), the dimension must be 3 or more.
- If non-linear differential equations are *integrable* $\rightarrow$ No chaos!
- One dimensional *discrete* systems (*logistic map*) can exhibit chaos.
- Well known book on mathematical aspects of chaos theory – Guckenheimer and Holmes (1983).

Introduction

Key Features of Chaotic Systems

- Main features of a chaotic system:
  - Sensitive dependence on initial conditions (see Duffing's equation) for certain parameter values.
  - Every point in phase space is *eventually visited* – Periodic system (single or finitely many periods), phase plot will *settle* in a region (see limit cycle in Duffing's equation).
  - Chaotic system, the *attractor* is *not* a *fixed point* or a *limit cycle* $\rightarrow$ *Strange attractor* has *fractal* dimension!
- Only in *non-linear* dynamical systems – Finite dimensional linear systems *can never* exhibit chaos.
- In *continuous* non-linear dynamical system (described by differential equation), the dimension must be 3 or more.
- If non-linear differential equations are *integrable* $\rightarrow$ No chaos!
- One dimensional *discrete* systems (*logistic map*) can exhibit chaos.
- Well known book on mathematical aspects of chaos theory – Guckenheimer and Holmes (1983).

Introduction

Key Features of Chaotic Systems

- Main features of a chaotic system:
  - Sensitive dependence on initial conditions (see Duffing's equation) for certain parameter values.
  - Every point in phase space is *eventually visited* – Periodic system (single or finitely many periods), phase plot will *settle* in a region (see limit cycle in Duffing's equation).
  - Chaotic system, the *attractor* is *not* a *fixed point* or a *limit cycle* $\rightarrow$ *Strange attractor* has *fractal* dimension!
- Only in *non-linear* dynamical systems – Finite dimensional linear systems *can never* exhibit chaos.
- In *continuous* non-linear dynamical system (described by differential equation), the dimension must be 3 or more.
- If non-linear differential equations are *integrable* $\rightarrow$ No chaos!
- One dimensional *discrete* systems (*logistic map*) can exhibit chaos.
- Well known book on mathematical aspects of chaos theory – Guckenheimer and Holmes (1983).

Introduction

Key Features of Chaotic Systems

- Main features of a chaotic system:
  - Sensitive dependence on initial conditions (see Duffing's equation) for certain parameter values.
  - Every point in phase space is *eventually visited* – Periodic system (single or finitely many periods), phase plot will *settle* in a region (see limit cycle in Duffing's equation).
  - Chaotic system, the *attractor* is *not* a *fixed point* or a *limit cycle* $\rightarrow$ *Strange attractor* has *fractal* dimension!
- Only in *non-linear* dynamical systems – Finite dimensional linear systems *can never* exhibit chaos.
- In *continuous* non-linear dynamical system (described by differential equation), the dimension must be 3 or more.
- If non-linear differential equations are *integrable* $\rightarrow$ No chaos!
- One dimensional *discrete* systems (*logistic map*) can exhibit chaos.
- Well known book on mathematical aspects of chaos theory – Guckenheimer and Holmes (1983).

Introduction

Key Features of Chaotic Systems

- Main features of a chaotic system:
  - Sensitive dependence on initial conditions (see Duffing's equation) for certain parameter values.
  - Every point in phase space is *eventually visited* – Periodic system (single or finitely many periods), phase plot will *settle* in a region (see limit cycle in Duffing's equation).
  - Chaotic system, the *attractor* is *not* a *fixed point* or a *limit cycle* $\rightarrow$ *Strange attractor* has *fractal* dimension!
- Only in *non-linear* dynamical systems – Finite dimensional linear systems *can never* exhibit chaos.
- In *continuous* non-linear dynamical system (described by differential equation), the dimension must be 3 or more.
- If non-linear differential equations are *integrable* $\rightarrow$ No chaos!
- One dimensional *discrete* systems (*logistic map*) can exhibit chaos.
- Well known book on mathematical aspects of chaos theory – Guckenheimer and Holmes (1983).

- Main features of a chaotic system:
  - Sensitive dependence on initial conditions (see Duffing's equation) for certain parameter values.
  - Every point in phase space is *eventually visited* – Periodic system (single or finitely many periods), phase plot will *settle* in a region (see limit cycle in Duffing's equation).
  - Chaotic system, the *attractor* is *not* a *fixed point* or a *limit cycle* $\rightarrow$ *Strange attractor* has *fractal* dimension!
- Only in *non-linear* dynamical systems – Finite dimensional linear systems *can never* exhibit chaos.
- In *continuous* non-linear dynamical system (described by differential equation), the dimension must be 3 or more.
- If non-linear differential equations are *integrable* $\rightarrow$ No chaos!
- One dimensional *discrete* systems (*logistic map*) can exhibit chaos.
- Well known book on mathematical aspects of chaos theory – Guckenheimer and Holmes (1983).

Robot Dynamics & Control

- Equations of motion of a robot are non-linear (see Module 6, Lecture 1)

$$[\mathbf{M}(\mathbf{q})]\ddot{\mathbf{q}} + \mathbf{C}(\mathbf{q},\dot{\mathbf{q}}) + \mathbf{G}(\mathbf{q}) + \mathbf{F}(\mathbf{q},\dot{\mathbf{q}}) = \tau$$

  - $[\mathbf{M}(\mathbf{q})]$ — Non-linear mass matrix – Trigonometric terms
  - $\mathbf{C}(\mathbf{q},\dot{\mathbf{q}})$ — Nonlinear Coriolis/Centripetal – trigonometric and quadratic products $\dot{q}_i\dot{q}_j$.
  - $\mathbf{G}(\mathbf{q})$ — Nonlinear gravity term – Trigonometric terms.
  - $\mathbf{F}(\mathbf{q},\dot{\mathbf{q}})$ — Nonlinear friction and other terms.
  - τ — Control torque/force at joints

- Control schemes are sometimes nonlinear.

- Equations of motion of a robot are non-linear (see Module 6, Lecture 1)

$$[\mathbf{M}(\mathbf{q})]\ddot{\mathbf{q}} + \mathbf{C}(\mathbf{q}, \dot{\mathbf{q}}) + \mathbf{G}(\mathbf{q}) + \mathbf{F}(\mathbf{q}, \dot{\mathbf{q}}) = \tau$$

  - $[\mathbf{M}(\mathbf{q})]$ — Non-linear mass matrix – Trigonometric terms
  - $\mathbf{C}(\mathbf{q}, \dot{\mathbf{q}})$ — Nonlinear Coriolis/Centripetal – trigonometric and quadratic products $\dot{q}_i \dot{q}_j$.
  - $\mathbf{G}(\mathbf{q})$ — Nonlinear gravity term – Trigonometric terms.
  - $\mathbf{F}(\mathbf{q}, \dot{\mathbf{q}})$ — Nonlinear friction and other terms.
  - τ — Control torque/force at joints
- Control schemes are sometimes nonlinear.

- To track a desired trajectory, various control schemes are used (see Module 7, Lecture 3).
- Proportional + Derivative(PD) or a PID control scheme

$$\tau_i = \ddot{q}_{d_i} + K_{p_i}(q_{d_i} - q_i) + K_{v_i}(\dot{q}_{d_i} - \dot{q}_i) + K_{I_i} \int (q_{d_i} - q_i) dt$$

- Model-based control schemes

$$\tau = [\widehat{\mathbf{M}(\mathbf{q})}]\tau' + \widehat{\mathbf{C}(\mathbf{q}, \dot{\mathbf{q}})} + \widehat{\mathbf{G}(\mathbf{q})} + \widehat{\mathbf{F}(\mathbf{q}, \dot{\mathbf{q}})}$$

  where τ' is same as in PD control scheme and $\widehat{(.)}$ are estimates used in model-based terms.
- PD and model-based control is *asymptotically* stable for a regulator problem under certain conditions (see Module 7, Lecture 3).
- Stability *not proved* for trajectory following with arbitrary $\mathbf{q}_d(t)$.

- To track a desired trajectory, various control schemes are used (see Module 7, Lecture 3).
- Proportional + Derivative(PD) or a PID control scheme

$$\tau_i = \ddot{q}_{d_i} + K_{p_i}(q_{d_i} - q_i) + K_{v_i}(\dot{q}_{d_i} - \dot{q}_i) + K_{I_i}\int (q_{d_i} - q_i)dt$$

- Model-based control schemes

$$\tau = \widehat{[\mathbf{M}(\mathbf{q})]}\tau' + \widehat{\mathbf{C}(\mathbf{q},\dot{\mathbf{q}})} + \widehat{\mathbf{G}(\mathbf{q})} + \widehat{\mathbf{F}(\mathbf{q},\dot{\mathbf{q}})}$$

  where τ' is same as in PD control scheme and $\widehat{(.)}$ are estimates used in model-based terms.
- PD and model-based control is *asymptotically* stable for a regulator problem under certain conditions (see Module 7, Lecture 3).
- Stability *not proved* for trajectory following with arbitrary $\mathbf{q}_d(t)$.

- To track a desired trajectory, various control schemes are used (see Module 7, Lecture 3).
- Proportional + Derivative(PD) or a PID control scheme

$$\tau_i = \ddot{q}_{d_i} + K_{p_i}(q_{d_i} - q_i) + K_{v_i}(\dot{q}_{d_i} - \dot{q}_i) + K_{I_i}\int (q_{d_i} - q_i)dt$$

- Model-based control schemes

$$\tau = [\widehat{\mathbf{M}(\mathbf{q})}]\tau' + \widehat{\mathbf{C}(\mathbf{q},\dot{\mathbf{q}})} + \widehat{\mathbf{G}(\mathbf{q})} + \widehat{\mathbf{F}(\mathbf{q},\dot{\mathbf{q}})}$$

where τ' is same as in PD control scheme and $\widehat{(.)}$ are estimates used in model-based terms.

- PD and model-based control is *asymptotically* stable for a regulator problem under certain conditions (see Module 7, Lecture 3).
- Stability *not proved* for trajectory following with arbitrary $\mathbf{q}_d(t)$.

- To track a desired trajectory, various control schemes are used (see Module 7, Lecture 3).
- Proportional + Derivative(PD) or a PID control scheme

$$\tau_i = \ddot{q}_{d_i} + K_{p_i}(q_{d_i} - q_i) + K_{v_i}(\dot{q}_{d_i} - \dot{q}_i) + K_{I_i}\int (q_{d_i} - q_i)dt$$

- Model-based control schemes

$$\tau = [\widehat{\mathbf{M}(\mathbf{q})}]\tau' + \widehat{\mathbf{C}(\mathbf{q}, \dot{\mathbf{q}})} + \widehat{\mathbf{G}(\mathbf{q})} + \widehat{\mathbf{F}(\mathbf{q}, \dot{\mathbf{q}})}$$

  where τ' is same as in PD control scheme and $\widehat{(.)}$ are estimates used in model-based terms.
- PD and model-based control is *asymptotically* stable for a regulator problem under certain conditions (see Module 7, Lecture 3).
- Stability *not proved* for trajectory following with arbitrary $\mathbf{q}_d(t)$.

- To track a desired trajectory, various control schemes are used (see Module 7, Lecture 3).
- Proportional + Derivative(PD) or a PID control scheme

$$\tau_i = \ddot{q}_{d_i} + K_{p_i}(q_{d_i} - q_i) + K_{v_i}(\dot{q}_{d_i} - \dot{q}_i) + K_{I_i}\int (q_{d_i} - q_i)dt$$

- Model-based control schemes

$$\tau = [\widehat{\mathbf{M}(\mathbf{q})}]\tau' + \widehat{\mathbf{C}(\mathbf{q},\dot{\mathbf{q}})} + \widehat{\mathbf{G}(\mathbf{q})} + \widehat{\mathbf{F}(\mathbf{q},\dot{\mathbf{q}})}$$

  where τ' is same as in PD control scheme and $\widehat{(.)}$ are estimates used in model-based terms.
- PD and model-based control is *asymptotically* stable for a regulator problem under certain conditions (see Module 7, Lecture 3).
- Stability *not proved* for trajectory following with arbitrary $\mathbf{q}_d(t)$.

- Equations of motion are $2\times$ DOF in number and non-autonomous.
- Simulation of 2 DOF robots – RR, RP, PR, and PP — 4 dimensional system!
- Assumptions
  - No gravity, friction and other non-linear terms.
  - Equation of motion contain *only* inertia and Coriolis/Centripetal Terms

$$[\mathbf{M}(\mathbf{q})]\ddot{\mathbf{q}} + \mathbf{C}(\mathbf{q},\dot{\mathbf{q}}) = \tau$$

  - Desired *repetitive* joint space trajectory – $q_{d\,i} = A_i \sin(\omega_i t), \quad i = 1,2$
  - Model estimates obtained by perturbing model parameters — multiply by $(1+\varepsilon)$
- Numerical integration of equations of motion with control laws.
- Observe evolution of state variables for various controller gains and estimates of model parameters.

- Equations of motion are $2\times$ DOF in number and non-autonomous.
- Simulation of 2 DOF robots – RR, RP, PR, and PP — 4 dimensional system!
- Assumptions
  - No gravity, friction and other non-linear terms.
  - Equation of motion contain *only* inertia and Coriolis/Centripetal Terms

$$[\mathbf{M}(\mathbf{q})]\ddot{\mathbf{q}} + \mathbf{C}(\mathbf{q},\dot{\mathbf{q}}) = \tau$$

  - Desired *repetitive* joint space trajectory – $q_{d_i} = A_i \sin(\omega_i t), \quad i = 1,2$
  - Model estimates obtained by perturbing model parameters — multiply by $(1+\varepsilon)$
- Numerical integration of equations of motion with control laws.
- Observe evolution of state variables for various controller gains and estimates of model parameters.

- Equations of motion are $2\times$ DOF in number and non-autonomous.
- Simulation of 2 DOF robots – RR, RP, PR, and PP — 4 dimensional system!
- Assumptions
  - No gravity, friction and other non-linear terms.
  - Equation of motion contain *only* inertia and Coriolis/Centripetal Terms

$$[\mathbf{M}(\mathbf{q})]\ddot{\mathbf{q}} + \mathbf{C}(\mathbf{q}, \dot{\mathbf{q}}) = \tau$$

  - Desired *repetitive* joint space trajectory – $q_{d\,i} = A_i \sin(\omega_i t), \quad i = 1, 2$
  - Model estimates obtained by perturbing model parameters — multiply by $(1+\varepsilon)$
- Numerical integration of equations of motion with control laws.
- Observe evolution of state variables for various controller gains and estimates of model parameters.

Robot Dynamics & Control

- Equations of motion are $2\times$ DOF in number and non-autonomous.
- Simulation of 2 DOF robots – RR, RP, PR, and PP — 4 dimensional system!
- Assumptions
  - No gravity, friction and other non-linear terms.
  - Equation of motion contain *only* inertia and Coriolis/Centripetal Terms

$$[\mathbf{M}(\mathbf{q})]\ddot{\mathbf{q}} + \mathbf{C}(\mathbf{q}, \dot{\mathbf{q}}) = \tau$$

  - Desired *repetitive* joint space trajectory – $q_{d\,i} = A_i \sin(\omega_i t), \quad i = 1, 2$
  - Model estimates obtained by perturbing model parameters — multiply by $(1+\varepsilon)$
- Numerical integration of equations of motion with control laws.
- Observe evolution of state variables for various controller gains and estimates of model parameters.

Robot Dynamics & Control

- Equations of motion are $2\times$ DOF in number and non-autonomous.
- Simulation of 2 DOF robots – RR, RP, PR, and PP — 4 dimensional system!
- Assumptions
  - No gravity, friction and other non-linear terms.
  - Equation of motion contain *only* inertia and Coriolis/Centripetal Terms

$$[\mathbf{M}(\mathbf{q})]\ddot{\mathbf{q}} + \mathbf{C}(\mathbf{q}, \dot{\mathbf{q}}) = \tau$$

  - Desired *repetitive* joint space trajectory – $q_{d\,i} = A_i \sin(\omega_i t), \quad i = 1, 2$
  - Model estimates obtained by perturbing model parameters — multiply by $(1+\varepsilon)$
- Numerical integration of equations of motion with control laws.
- Observe evolution of state variables for various controller gains and estimates of model parameters.

Diagnostic Tools for Chaos

- Phase plots – Plot of position Vs. velocity
  - Non-chaotic – Closed with one or more but finite number of loops.
  - Chaotic – Not closed and fills up a region in phase space.
- Lyapunov exponents – Measures divergence of adjacent trajectories as $t \to \infty$ (see Parker and Chua (1989), Wolf et al. (1985)).
  - n exponents for n dimensional system – one exponent is zero always.
  - At least one positive for chaotic system.
- Poincaré maps — Stroboscopic sampling of phase plots
  - One or finite number of points in non-chaotic case
  - Points tend to fill up a region — Strange Attractor.
- Bifurcation diagrams
  - Plot of a state variables as a parameter is varied.
  - Pre- and post-chaotic behavior.

Diagnostic Tools for Chaos

- Phase plots – Plot of position Vs. velocity
  - Non-chaotic – Closed with one or more but finite number of loops.
  - Chaotic – Not closed and fills up a region in phase space.
- Lyapunov exponents – Measures divergence of adjacent trajectories as $t \to \infty$ (see Parker and Chua (1989), Wolf et al. (1985)).
  - n exponents for n dimensional system – one exponent is zero always.
  - At least one positive for chaotic system.
- Poincaré maps — Stroboscopic sampling of phase plots
  - One or finite number of points in non-chaotic case
  - Points tend to fill up a region — Strange Attractor.
- Bifurcation diagrams
  - Plot of a state variables as a parameter is varied.
  - Pre- and post-chaotic behavior.

Diagnostic Tools for Chaos

- Phase plots – Plot of position Vs. velocity
  - Non-chaotic – Closed with one or more but finite number of loops.
  - Chaotic – Not closed and fills up a region in phase space.
- Lyapunov exponents – Measures divergence of adjacent trajectories as $t \to \infty$ (see Parker and Chua (1989), Wolf et al. (1985)).
  - n exponents for n dimensional system – one exponent is zero always.
  - At least one positive for chaotic system.
- Poincaré maps — Stroboscopic sampling of phase plots
  - One or finite number of points in non-chaotic case
  - Points tend to fill up a region — Strange Attractor.
- Bifurcation diagrams
  - Plot of a state variables as a parameter is varied.
  - Pre- and post-chaotic behavior.

Diagnostic Tools for Chaos

- Phase plots – Plot of position Vs. velocity
  - Non-chaotic – Closed with one or more but finite number of loops.
  - Chaotic – Not closed and fills up a region in phase space.
- Lyapunov exponents – Measures divergence of adjacent trajectories as $t \to \infty$ (see Parker and Chua (1989), Wolf et al. (1985)).
  - n exponents for n dimensional system – one exponent is zero always.
  - At least one positive for chaotic system.
- Poincaré maps — Stroboscopic sampling of phase plots
  - One or finite number of points in non-chaotic case
  - Points tend to fill up a region — Strange Attractor.
- Bifurcation diagrams
  - Plot of a state variables as a parameter is varied.
  - Pre- and post-chaotic behavior.

Simulation Results

The RP manipulator

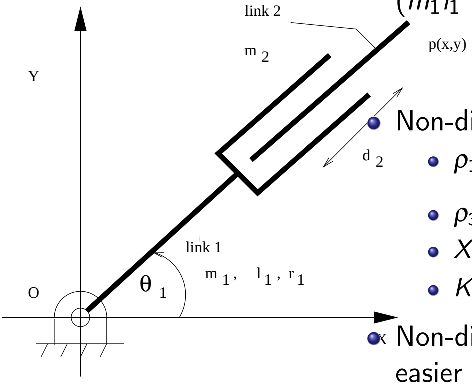

Figure 5: The RP Manipulator

- Equations of motion

$$(m_1 l_1{}^2 + I_1 + I_2 + m_2 d_2{}^2)\ddot{\theta}_1 + 2 m_2 d_2 \dot{\theta}_1 \dot{d}_2 = \tau_1$$

$$m_2 \ddot{d}_2 - m_2 d_2 \dot{\theta}_1{}^2 = F_2$$

- Non-dimensional parameters
  - $\rho_1 = (1 + \frac{I_1 + I_2}{m_1 l_1^2})$, $\rho_2 = \frac{m_2}{m_1}$
  - $\rho_3 = \frac{m_1 l_1^2}{1.0}$, $\rho_4 = \frac{m_1 l_1}{1.0}$
  - $X = \frac{d_2}{l_1}$, $\tau_1^* = \frac{\tau_1}{\rho_3}$, $F_2^* = \frac{F_2}{\rho_4}$
  - $K_p^* = K_p/\omega^2$, $K_v^* = K_v/\omega$, $t^* = \omega t$
- Non-dimensional parameters are fewer!! $\rightarrow$ easier to search parameter space for obtaining chaotic behaviour.
- For model based control $\hat{\rho}_i = (1 + \varepsilon)\rho_i$

Simulation Results

The RP manipulator under PD Control

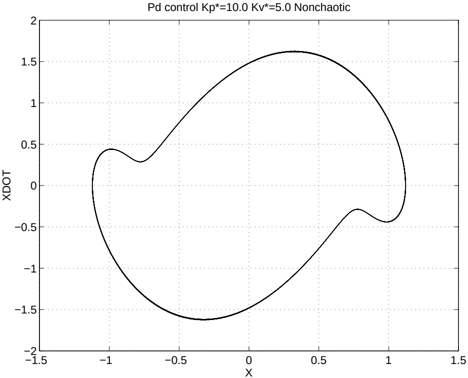

Figure 6: Phase plot in non-chaotic case

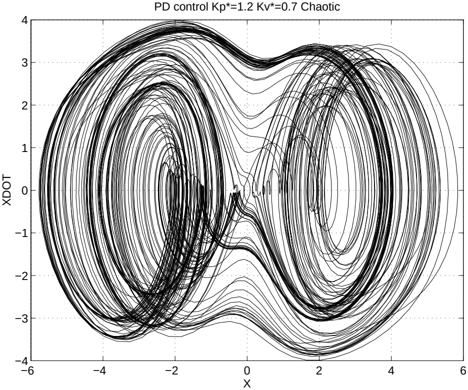

Figure 7: Phase plot in chaotic case[From Ravishankar and Ghosal (1999)]

- $A_\theta = \pi, \quad A_X = 1.0$ and $\omega = 1.0$
- Non-dimensional parameters – $\rho_1 = 2.5$, $\rho_2 = 0.5$, $\rho_3 = 0.4$, and $\rho_4 = 2.0$.

Simulation Results

The RP manipulator under PD Control

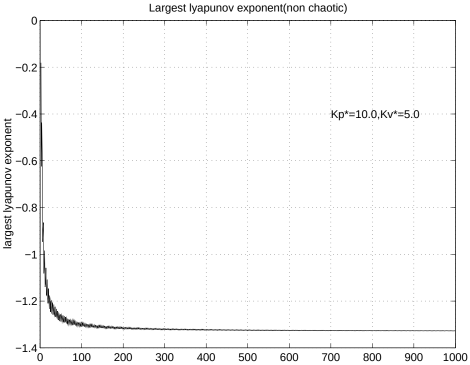

Figure 8: Lyapunov exponent in non-chaotic case

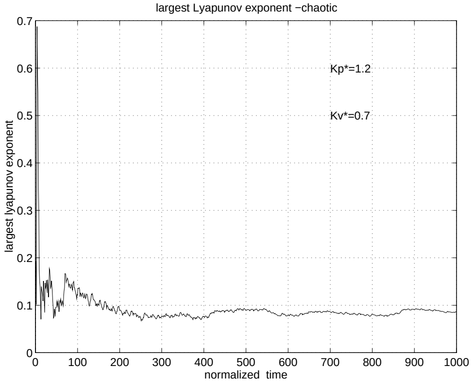

Figure 9: Lyapunov exponent in chaotic case

- Largest Lyapunov exponent for chaotic and non-chaotic cases.
- $A_\theta = \pi$, $A_X = 1.0$, $\omega = 1.0$, $\rho_1 = 2.5$, $\rho_2 = 0.5$, and $\rho_3 = 0.4$, $\rho_4 = 2.0$

Simulation Results

The RP manipulator under PD Control

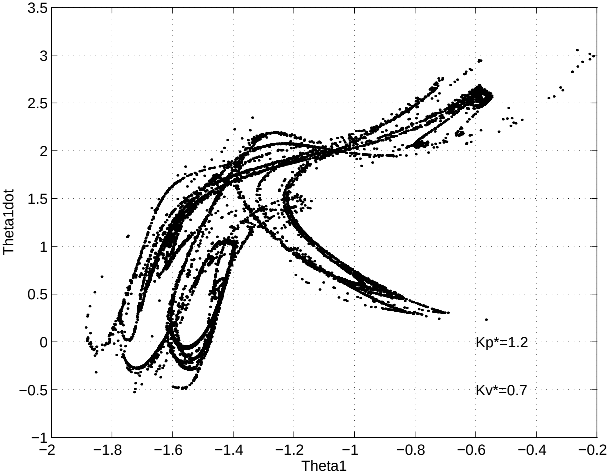

Figure 10: Poincaré map for RP manipulator under PD control

- Poincaré map
- $(\dot{\theta}_1, \theta_1)$ projection.
- $A_\theta = \pi$, $A_X = 1.0$, $\omega = 1.0$, $\rho_1 = 2.5$, $\rho_2 = 0.5$, and $\rho_3 = 0.4$,

The RP manipulator under PD and Model-based Control

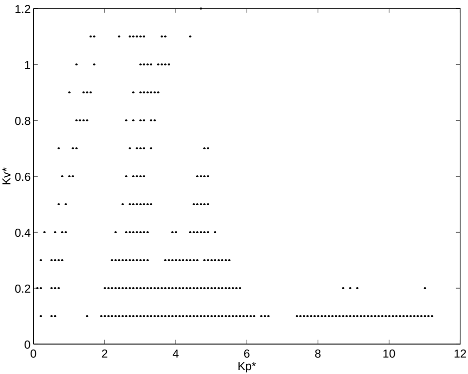

Figure 11: Chaos maps for RP manipulator under PD control

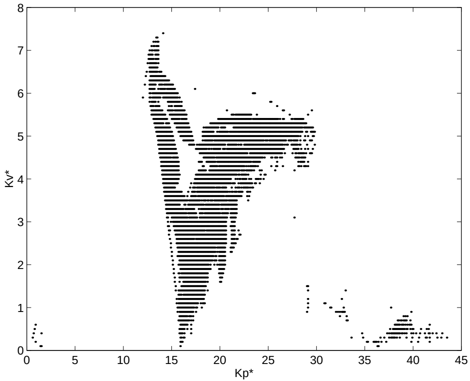

Figure 12: Chaos maps for RP manipulator under model-based control

- Chaos maps – values of gains for chaotic behavior.
- K_v^* in steps of 0.1, K_p^* in steps of 1.0.
- Initial conditions – $(0, 0, \pi, 1.0)$

Simulation Results

The RP manipulator under PD and Model-based Control

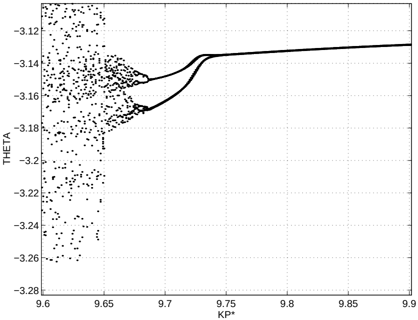

Figure 13: Bifurcation diagram for RP manipulator under PD control

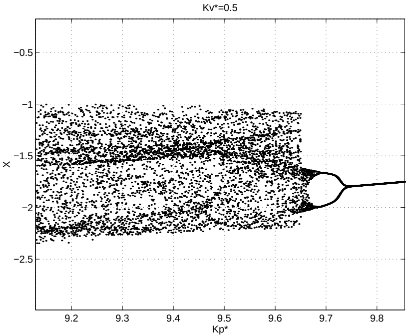

Figure 14: Bifurcation diagram for RP manipulator under model-based control

- Bifurcation diagrams – Plot of state-variable as K_p^* is changed at a fixed K_v^*.
- Period doubling route to chaos!

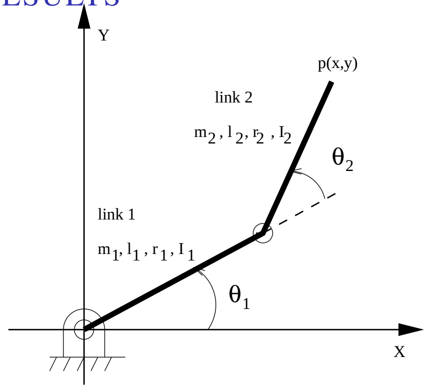

Figure 15: The RR Manipulator

- Equations of motion (see Module 6, Lecture 2)

$$(m_1 r_1^2 + I_1 + m_2 r_2^2 + I_2 + m_2 l_1^2 + 2 m_2 l_1 r_2 \cos\theta_2)\ddot{\theta}_1 +$$
$$(m_2 r_2^2 + I_2 + m_2 l_1 r_2 \cos\theta_2)\ddot{\theta}_2 - m_2 l_1 r_2 \sin\theta_2 (2\dot{\theta}_1 + \dot{\theta}_2)\dot{\theta}_2 = \tau_1$$
$$(m_2 r_2^2 + I_2 + m_2 l_1 r_2 \cos\theta_2)\ddot{\theta}_1 + (m_2 r_2^2 + I_2)\ddot{\theta}_2 + m_2 l_1 r_2 \sin\theta_2 \dot{\theta}_1^2 = \tau_2$$

- The RR manipulator (or a double pendulum) is known to be chaotic (see Mahout et al. (1993)).

Simulation Results

The RR manipulator under PD and model-based control

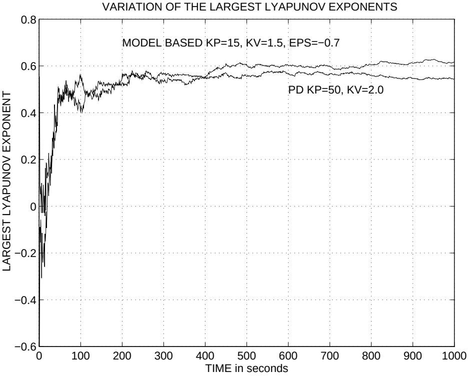

Figure 16: Largest Lyapunov exponent for the RR manipulator under PD and model-based control

- $A_{\theta_1} = \pi/2, \quad A_{\theta_2} = \pi/4$ and $\omega = 2.0$
- Mass and DH parameters – Correspond to the first two links of the CMU DD Arm II (see Khosla (1986))

Simulation Results

The RR manipulator under PD and model-based control

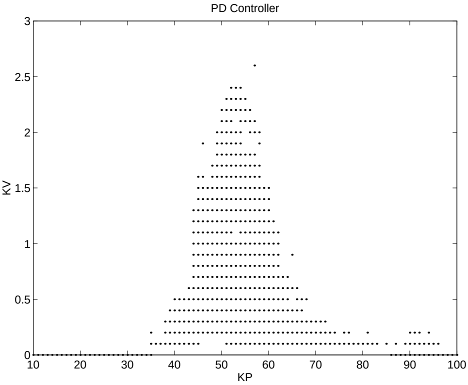

Figure 17: Chaos map for PD control of the RR Manipulator

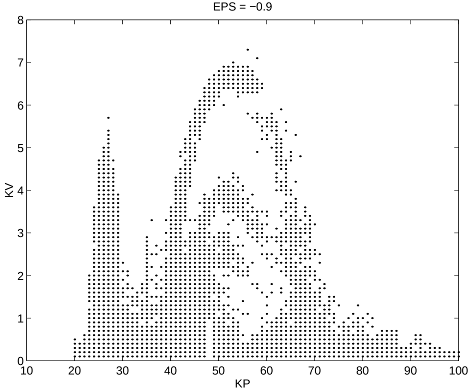

Figure 18: Chaos map for model-based control of the RR Manipulator

- K_v^* in steps of 0.1, K_p^* in steps of 1.0
- Initial conditions – $(0, \pi, 0, \pi/2)$, $\epsilon = -0.9$

Simulation Results

The RR manipulator under model-based control

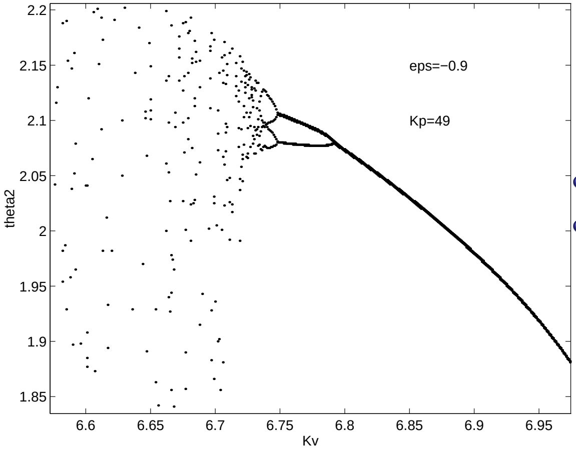

Figure 19: Bifurcation diagram for RR manipulator

- $\varepsilon = -0.9$ and $K_p = 49$
- Period doubling route to chaos

Simulation Results
Summary

- Numerical simulation of 2 DOF planar robots under PD and model-based controller.
- Both the RR and RP robot can exhibit chaotic motions
  - Chaotic motions for low controller gains
  - Chaotic motions for large mismatch between model and plant
  - Chaotic motions seen more easily for underestimations
- Route to chaos appear to be through period doubling.
- PR and PP robot *do not* show chaotic motions even after extensive simulations!

- Numerical simulation of 2 DOF planar robots under PD and model-based controller.
- Both the RR and RP robot can exhibit chaotic motions
  - Chaotic motions for low controller gains
  - Chaotic motions for large mismatch between model and plant
  - Chaotic motions seen more easily for underestimations
- Route to chaos appear to be through period doubling.
- PR and PP robot *do not* show chaotic motions even after extensive simulations!

Simulation Results

Summary

- Numerical simulation of 2 DOF planar robots under PD and model-based controller.
- Both the RR and RP robot can exhibit chaotic motions
  - Chaotic motions for low controller gains
  - Chaotic motions for large mismatch between model and plant
  - Chaotic motions seen more easily for underestimations
- Route to chaos appear to be through period doubling.
- PR and PP robot *do not* show chaotic motions even after extensive simulations!

- Numerical simulation of 2 DOF planar robots under PD and model-based controller.
- Both the RR and RP robot can exhibit chaotic motions
    - Chaotic motions for low controller gains
    - Chaotic motions for large mismatch between model and plant
    - Chaotic motions seen more easily for underestimations
- Route to chaos appear to be through period doubling.
- PR and PP robot *do not* show chaotic motions even after extensive simulations!

ANALYTICAL CRITERIA

- The manipulator mass matrix, $[\mathbf{M}(\mathbf{q})]$, is positive definite.
- $[\mathbf{M}(\mathbf{q})]$ defines a Riemannian metric in the *configuration space* $(\mathbf{q})$
- From $[\mathbf{M}(\mathbf{q})]$ one can compute Riemannian curvature tensor

$$R_{ijkl} = \sum_{h=1}^{n} M_{ih} R_{ikl}^{h}$$

- Equations of motion in absence of potential energy

$$\dot{\mathbf{q}} = \frac{\partial H}{\partial \mathbf{p}}, \quad \dot{\mathbf{p}} = -\frac{\partial H}{\partial \mathbf{q}} + \tau$$

$\mathbf{p}$ is the momentum and $H(\mathbf{p}, \mathbf{q})$ is the Hamiltonian of the system.

Analytical Criteria

- The manipulator mass matrix, $[\mathbf{M}(\mathbf{q})]$, is positive definite.
- $[\mathbf{M}(\mathbf{q})]$ defines a Riemannian metric in the *configuration space* $(\mathbf{q})$
- From $[\mathbf{M}(\mathbf{q})]$ one can compute Riemannian curvature tensor

$$R_{ijkl} = \sum_{h=1}^{n} M_{ih} R^{h}_{jkl}$$

- Equations of motion in absence of potential energy

$$\dot{\mathbf{q}} = \frac{\partial H}{\partial \mathbf{p}}, \quad \dot{\mathbf{p}} = -\frac{\partial H}{\partial \mathbf{q}} + \tau$$

$\mathbf{p}$ is the momentum and $H(\mathbf{p}, \mathbf{q})$ is the Hamiltonian of the system.

Analytical Criteria

- The manipulator mass matrix, $[\mathbf{M}(\mathbf{q})]$, is positive definite.
- $[\mathbf{M}(\mathbf{q})]$ defines a Riemannian metric in the *configuration space* $(\mathbf{q})$
- From $[\mathbf{M}(\mathbf{q})]$ one can compute Riemannian curvature tensor

$$R_{ijkl} = \sum_{h=1}^{n} M_{ih} R^{h}_{ikl}$$

- Equations of motion in absence of potential energy

$$\dot{\mathbf{q}} = \frac{\partial H}{\partial \mathbf{p}}, \quad \dot{\mathbf{p}} = -\frac{\partial H}{\partial \mathbf{q}} + \tau$$

$\mathbf{p}$ is the momentum and $H(\mathbf{p}, \mathbf{q})$ is the Hamiltonian of the system.

Analytical Criteria

- The manipulator mass matrix, $[\mathbf{M}(\mathbf{q})]$, is positive definite.
- $[\mathbf{M}(\mathbf{q})]$ defines a Riemannian metric in the *configuration space* ($\mathbf{q}$)
- From $[\mathbf{M}(\mathbf{q})]$ one can compute Riemannian curvature tensor

$$R_{ijkl} = \sum_{h=1}^{n} M_{ih} R^{h}_{ikl}$$

- Equations of motion in absence of potential energy

$$\dot{\mathbf{q}} = \frac{\partial H}{\partial \mathbf{p}}, \quad \dot{\mathbf{p}} = -\frac{\partial H}{\partial \mathbf{q}} + \tau$$

$\mathbf{p}$ is the momentum and $H(\mathbf{p}, \mathbf{q})$ is the Hamiltonian of the system.

Analytical Criteria (Contd.)

- If $R_{ijkl} = 0$, then the mass matrix can be factorized

$$[\mathbf{M}(\mathbf{q})] = [N(\mathbf{q})]^T [N(\mathbf{q})]$$

$[N(\mathbf{q})]$ is integrable(Stoker 1969, Spong 1992).

- Equations of motion can be written as

$$\dot{\mathbf{q}} = \mathbf{P}, \quad \dot{\mathbf{P}} = [N(\mathbf{q})]^{-T} \tau$$

- For $\tau = 0 \Rightarrow$ Equations of motion *can be integrated* in closed-form $\Rightarrow$ *Cannot* exhibit chaos!
- Can obtain R_{ijkl} easily for 2 DOF robots since $[\mathbf{M}(\mathbf{q})]$ is known.
- If $R_{ijkl} = 0$ then chaotic motion not possible.
- Not required to compute full tensor R_{ijkl} – Gaussian curvature of 2D subspace enough!

Analytical Criteria (Contd.)

- If $R_{ijkl} = 0$, then the mass matrix can be factorized

$$[\mathbf{M}(\mathbf{q})] = [N(\mathbf{q})]^T [N(\mathbf{q})]$$

  $[N(\mathbf{q})]$ is integrable(Stoker 1969, Spong 1992).

- Equations of motion can be written as

$$\dot{\mathbf{q}} = \mathbf{P}, \quad \dot{\mathbf{P}} = [N(\mathbf{q})]^{-T} \tau$$

- For $\tau = 0 \Rightarrow$ Equations of motion *can be integrated* in closed-form $\Rightarrow$ *Cannot* exhibit chaos!
- Can obtain R_{ijkl} easily for 2 DOF robots since $[\mathbf{M}(\mathbf{q})]$ is known.
- If $R_{ijkl} = 0$ then chaotic motion not possible.
- Not required to compute full tensor R_{ijkl} – Gaussian curvature of 2D subspace enough!

Analytical Criteria (Contd.)

- If $R_{ijkl} = 0$, then the mass matrix can be factorized

$$[\mathbf{M}(\mathbf{q})] = [N(\mathbf{q})]^T [N(\mathbf{q})]$$

  $[N(\mathbf{q})]$ is integrable(Stoker 1969, Spong 1992).

- Equations of motion can be written as

$$\dot{\mathbf{q}} = \mathbf{P}, \quad \dot{\mathbf{P}} = [N(\mathbf{q})]^{-T} \tau$$

- For $\tau = 0 \Rightarrow$ Equations of motion *can be integrated* in closed-form $\Rightarrow$ *Cannot* exhibit chaos!
- Can obtain R_{ijkl} easily for 2 DOF robots since $[\mathbf{M}(\mathbf{q})]$ is known.
- If $R_{ijkl} = 0$ then chaotic motion not possible.
- Not required to compute full tensor R_{ijkl} – Gaussian curvature of 2D subspace enough!

Analytical Criteria (Contd.)

- If $R_{ijkl} = 0$, then the mass matrix can be factorized

$$[\mathbf{M}(\mathbf{q})] = [N(\mathbf{q})]^T [N(\mathbf{q})]$$

  $[N(\mathbf{q})]$ is integrable(Stoker 1969, Spong 1992).
- Equations of motion can be written as

$$\dot{\mathbf{q}} = \mathbf{P}, \quad \dot{\mathbf{P}} = [N(\mathbf{q})]^{-T} \tau$$

- For $\tau = 0 \Rightarrow$ Equations of motion *can be integrated* in closed-form $\Rightarrow$ *Cannot* exhibit chaos!
- Can obtain R_{ijkl} easily for 2 DOF robots since $[\mathbf{M}(\mathbf{q})]$ is known.
- If $R_{ijkl} = 0$ then chaotic motion not possible.
- Not required to compute full tensor R_{ijkl} – Gaussian curvature of 2D subspace enough!

Analytical Criteria (Contd.)

- If $R_{ijkl} = 0$, then the mass matrix can be factorized

$$[\mathbf{M}(\mathbf{q})] = [N(\mathbf{q})]^T [N(\mathbf{q})]$$

  $[N(\mathbf{q})]$ is integrable(Stoker 1969, Spong 1992).

- Equations of motion can be written as

$$\dot{\mathbf{q}} = \mathbf{P}, \quad \dot{\mathbf{P}} = [N(\mathbf{q})]^{-T} \tau$$

- For $\tau = 0 \Rightarrow$ Equations of motion *can be integrated* in closed-form $\Rightarrow$ *Cannot* exhibit chaos!
- Can obtain R_{ijkl} easily for 2 DOF robots since $[\mathbf{M}(\mathbf{q})]$ is known.
- If $R_{ijkl} = 0$ then chaotic motion not possible.
- Not required to compute full tensor R_{ijkl} – Gaussian curvature of 2D subspace enough!

Analytical Criteria (Contd.)

- If $R_{ijkl} = 0$, then the mass matrix can be factorized

$$[\mathbf{M}(\mathbf{q})] = [N(\mathbf{q})]^T [N(\mathbf{q})]$$

  $[N(\mathbf{q})]$ is integrable(Stoker 1969, Spong 1992).
- Equations of motion can be written as

$$\dot{\mathbf{q}} = \mathbf{P}, \quad \dot{\mathbf{P}} = [N(\mathbf{q})]^{-T} \tau$$

- For $\tau = 0 \Rightarrow$ Equations of motion *can be integrated* in closed-form $\Rightarrow$ *Cannot* exhibit chaos!
- Can obtain R_{ijkl} easily for 2 DOF robots since $[\mathbf{M}(\mathbf{q})]$ is known.
- If $R_{ijkl} = 0$ then chaotic motion not possible.
- Not required to compute full tensor R_{ijkl} – Gaussian curvature of 2D subspace enough!

Analytical Criteria (contd.)

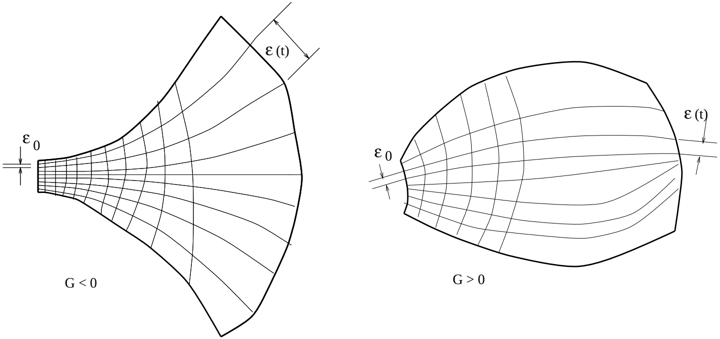

Figure 20: Gaussian curvature and trajectories

- $\tau = 0$ – Trajectories along *geodesics* of manifold (Arnold 1989).
- $R_{ijkl} \neq 0 \rightarrow$ Gaussian curvature of 2D subspace – $G = (R_{1212}/\det[\mathbf{M}])$
- In figures aboves, $\varepsilon(t) = \varepsilon_0 e^{\sqrt{-G}t}$
- $G < 0 \rightarrow$ nearby trajectories diverge *exponentially* — Chaos!
- Analytical criteria — $G < 0$ in any 2D subspace $\rightarrow$ Chaotic (see also Zak (1985a & b)).

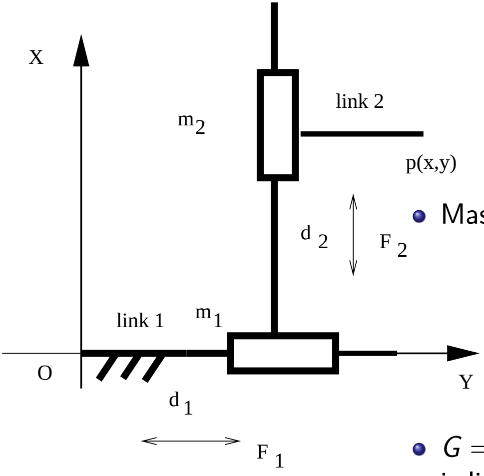

Figure 21: The PP Robot

- $KE = \frac{1}{2} m_1 \dot{d_1}^2 + \frac{1}{2} m_2 \dot{d_2}^2$
- Elements of the mass matrix

$$M_{11} = m_1, \quad M_{12} = 0, \quad M_{22} = m_2$$

- Mass matrix is constant.
- $G = 0 \rightarrow$ Not chaotic – Expected as it is linear system!

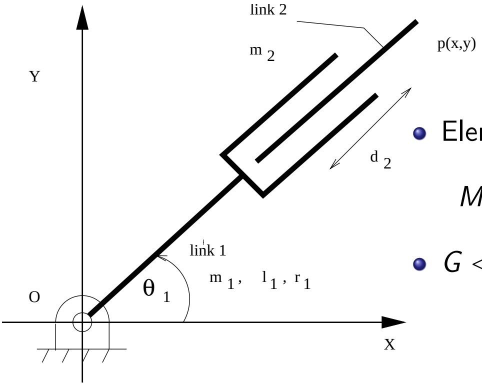

Figure 22: The RP Robot

- Elements of mass matrix

$$M_{11} = I + m_2 d_2^2, \;\; M_{12} = 0, \;\; M_{22} = m_2$$

- $G < 0$ for $I > 0 \rightarrow$ Always chaotic!

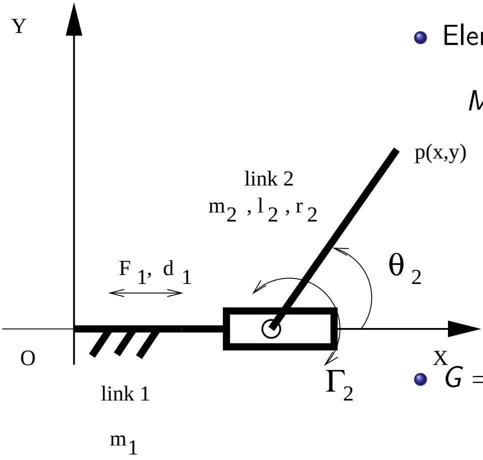

Figure 23: The PR Robot

- Elements of mass matrix

$$M_{11} = m_1 + m_2, \ M_{12} = -m_2 r_2 \sin\theta_2$$

$$M_{22} = m_2 r_2^2 + I_2$$

- $G = 0 \rightarrow$ Not chaotic!

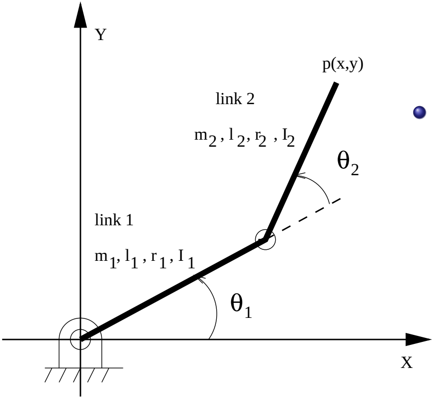

Figure 24: The RR Robot

- Elements of mass matrix

$$M_{11} = c_1 + c_2 \cos\theta_2$$

$$M_{12} = 2(c_3 + c_4 \cos\theta_2), \; M_{22} = c_3$$

$c_i, \; i = 1,2,3,4$ are constants.

- $G < 0$ if $\cos\theta_2 < -\dfrac{a_2c_1 - b_1 + 2a_3c_3 - a_4c_1 + 2a_5c_3}{a_1 + a_2c_2 + 2a_3c_4 - a_4c_2 + 2a_5c_4}$, $a_i, \; i = 1,2,3,4$ constants.
- Conditionally chaotic.

Analytical Criteria

- Gaussian curvature is zero for PP and PR robots $\rightarrow$ PP and PR manipulators do not show chaotic behaviour.
- Gaussian curvature is less than zero for RR and RP robots $\rightarrow$ Shows chaotic behaviour in numerical simulation.
- Gaussian curvature of a 2D subspace less than zero for RRR and RRP robots.
- Negative Gaussian curvature criteria is for *unforced motion*.
- Numerical simulation and Lyapunov exponent or other diagnostic criteria needs to be used for forced and/or controlled motion.

ANALYTICAL CRITERIA

- Gaussian curvature is zero for PP and PR robots $\rightarrow$ PP and PR manipulators do not show chaotic behaviour.
- Gaussian curvature is less than zero for RR and RP robots $\rightarrow$ Shows chaotic behaviour in numerical simulation.
- Gaussian curvature of a 2D subspace less than zero for RRR and RRP robots.
- Negative Gaussian curvature criteria is for *unforced motion*.
- Numerical simulation and Lyapunov exponent or other diagnostic criteria needs to be used for forced and/or controlled motion.

Analytical Criteria

- Gaussian curvature is zero for PP and PR robots $\rightarrow$ PP and PR manipulators do not show chaotic behaviour.
- Gaussian curvature is less than zero for RR and RP robots $\rightarrow$ Shows chaotic behaviour in numerical simulation.
- Gaussian curvature of a 2D subspace less than zero for RRR and RRP robots.
- Negative Gaussian curvature criteria is for *unforced motion*.
- Numerical simulation and Lyapunov exponent or other diagnostic criteria needs to be used for forced and/or controlled motion.

Analytical Criteria

- Gaussian curvature is zero for PP and PR robots $\rightarrow$ PP and PR manipulators do not show chaotic behaviour.
- Gaussian curvature is less than zero for RR and RP robots $\rightarrow$ Shows chaotic behaviour in numerical simulation.
- Gaussian curvature of a 2D subspace less than zero for RRR and RRP robots.
- Negative Gaussian curvature criteria is for *unforced motion*.
- Numerical simulation and Lyapunov exponent or other diagnostic criteria needs to be used for forced and/or controlled motion.

ANALYTICAL CRITERIA

- Gaussian curvature is zero for PP and PR robots $\rightarrow$ PP and PR manipulators do not show chaotic behaviour.
- Gaussian curvature is less than zero for RR and RP robots $\rightarrow$ Shows chaotic behaviour in numerical simulation.
- Gaussian curvature of a 2D subspace less than zero for RRR and RRP robots.
- Negative Gaussian curvature criteria is for *unforced motion*.
- Numerical simulation and Lyapunov exponent or other diagnostic criteria needs to be used for forced and/or controlled motion.

SUMMARY

- Robot dynamic and control equations are non-linear ODE's.
- Nonlinearity different from nonlinear spring or other commonly studied chaotic systems.
- Equations are higher dimensional and more complicated than commonly studied ones.
- Feedback control equations for robots can exhibit chaos.
- Suggest a re-look at some of the robustness results in robot control (see Craig (1989)).
- Lower bounds on controller gains can be obtained by numerical simulations.
- For *unforced motion* negative Gaussian curvature criteria may be useful.

Summary

- Robot dynamic and control equations are non-linear ODE's.
- Nonlinearity different from nonlinear spring or other commonly studied chaotic systems.
- Equations are higher dimensional and more complicated than commonly studied ones.
- Feedback control equations for robots can exhibit chaos.
- Suggest a re-look at some of the robustness results in robot control (see Craig (1989)).
- Lower bounds on controller gains can be obtained by numerical simulations.
- For *unforced motion* negative Gaussian curvature criteria may be useful.

SUMMARY

- Robot dynamic and control equations are non-linear ODE's.
- Nonlinearity different from nonlinear spring or other commonly studied chaotic systems.
- Equations are higher dimensional and more complicated than commonly studied ones.
- Feedback control equations for robots can exhibit chaos.
- Suggest a re-look at some of the robustness results in robot control (see Craig (1989)).
- Lower bounds on controller gains can be obtained by numerical simulations.
- For *unforced motion* negative Gaussian curvature criteria may be useful.

SUMMARY

- Robot dynamic and control equations are non-linear ODE's.
- Nonlinearity different from nonlinear spring or other commonly studied chaotic systems.
- Equations are higher dimensional and more complicated than commonly studied ones.
- Feedback control equations for robots can exhibit chaos.
- Suggest a re-look at some of the robustness results in robot control (see Craig (1989)).
- Lower bounds on controller gains can be obtained by numerical simulations.
- For *unforced motion* negative Gaussian curvature criteria may be useful.

SUMMARY

- Robot dynamic and control equations are non-linear ODE's.
- Nonlinearity different from nonlinear spring or other commonly studied chaotic systems.
- Equations are higher dimensional and more complicated than commonly studied ones.
- Feedback control equations for robots can exhibit chaos.
- Suggest a re-look at some of the robustness results in robot control (see Craig (1989)).
- Lower bounds on controller gains can be obtained by numerical simulations.
- For *unforced motion* negative Gaussian curvature criteria may be useful.

SUMMARY

- Robot dynamic and control equations are non-linear ODE's.
- Nonlinearity different from nonlinear spring or other commonly studied chaotic systems.
- Equations are higher dimensional and more complicated than commonly studied ones.
- Feedback control equations for robots can exhibit chaos.
- Suggest a re-look at some of the robustness results in robot control (see Craig (1989)).
- Lower bounds on controller gains can be obtained by numerical simulations.
- For *unforced motion* negative Gaussian curvature criteria may be useful.

SUMMARY

- Robot dynamic and control equations are non-linear ODE's.
- Nonlinearity different from nonlinear spring or other commonly studied chaotic systems.
- Equations are higher dimensional and more complicated than commonly studied ones.
- Feedback control equations for robots can exhibit chaos.
- Suggest a re-look at some of the robustness results in robot control (see Craig (1989)).
- Lower bounds on controller gains can be obtained by numerical simulations.
- For *unforced motion* negative Gaussian curvature criteria may be useful.

OUTLINE

Contents of Lecture[3]

- Introduction
- Kinematics and statics of Gough-Stewart platform.
- Isotropic and singular configurations
- Six component force-torque sensors based on a Gough-Stewart platform at a near singular configuration.
- Modeling, analysis and design of Gough-Stewart platform based sensors.
- Hardware and experimental results.
- Summary

[3] Major portions of this Lecture are from Bandyopadhyay & Ghosal (2006, 2008 & 2009) and Ranganath et. al (2004). Please see these and references listed at the end for more details.

Contents of Lecture[3]

- Introduction
- Kinematics and statics of Gough-Stewart platform.
- Isotropic and singular configurations
- Six component force-torque sensors based on a Gough-Stewart platform at a near singular configuration.
- Modeling, analysis and design of Gough-Stewart platform based sensors.
- Hardware and experimental results.
- Summary

[3]Major portions of this Lecture are from Bandyopadhyay & Ghosal (2006, 2008 & 2009) and Ranganath et. al (2004). Please see these and references listed at the end for more details.

CONTENTS OF LECTURE[3]

- Introduction
- Kinematics and statics of Gough-Stewart platform.
- Isotropic and singular configurations
- Six component force-torque sensors based on a Gough-Stewart platform at a near singular configuration.
- Modeling, analysis and design of Gough-Stewart platform based sensors.
- Hardware and experimental results.
- Summary

[3] Major portions of this Lecture are from Bandyopadhyay & Ghosal (2006, 2008 & 2009) and Ranganath et. al (2004). Please see these and references listed at the end for more details.

Contents of Lecture[3]

- Introduction
- Kinematics and statics of Gough-Stewart platform.
- Isotropic and singular configurations
- Six component force-torque sensors based on a Gough-Stewart platform at a near singular configuration.
- Modeling, analysis and design of Gough-Stewart platform based sensors.
- Hardware and experimental results.
- Summary

[3]Major portions of this Lecture are from Bandyopadhyay & Ghosal (2006, 2008 & 2009) and Ranganath et. al (2004). Please see these and references listed at the end for more details.

Contents of Lecture[3]

- Introduction
- Kinematics and statics of Gough-Stewart platform.
- Isotropic and singular configurations
- Six component force-torque sensors based on a Gough-Stewart platform at a near singular configuration.
- Modeling, analysis and design of Gough-Stewart platform based sensors.
- Hardware and experimental results.
- Summary

[3] Major portions of this Lecture are from Bandyopadhyay & Ghosal (2006, 2008 & 2009) and Ranganath et. al (2004). Please see these and references listed at the end for more details.

CONTENTS OF LECTURE[3]

- Introduction
- Kinematics and statics of Gough-Stewart platform.
- Isotropic and singular configurations
- Six component force-torque sensors based on a Gough-Stewart platform at a near singular configuration.
- Modeling, analysis and design of Gough-Stewart platform based sensors.
- Hardware and experimental results.
- Summary

[3]Major portions of this Lecture are from Bandyopadhyay & Ghosal (2006, 2008 & 2009) and Ranganath et. al (2004). Please see these and references listed at the end for more details.

Contents of Lecture[3]

- Introduction
- Kinematics and statics of Gough-Stewart platform.
- Isotropic and singular configurations
- Six component force-torque sensors based on a Gough-Stewart platform at a near singular configuration.
- Modeling, analysis and design of Gough-Stewart platform based sensors.
- Hardware and experimental results.
- Summary

[3] Major portions of this Lecture are from Bandyopadhyay & Ghosal (2006, 2008 & 2009) and Ranganath et. al (2004). Please see these and references listed at the end for more details.

INTRODUCTION

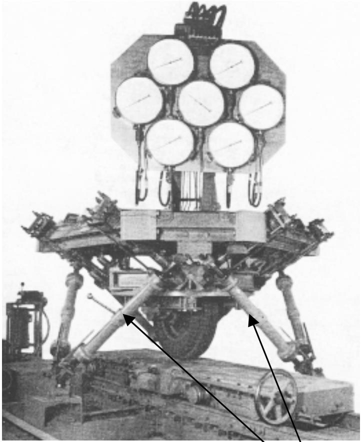

Stewart 1965

Extendable `legs'

Figure 25: The Stewart platform (Stewart 1965)

- First used as tyre testing machine in UK.
- Now known as Gough-Stewart platform.
- A moving platform connected to fixed ground by six actuated extendable legs — 6 DOF (Fichter 1986)
- Linear motion of platform along X, Y and Z axes & Rotational motion about X, Y and Z axes.
- Known also as Heave, Surge, Sway & Roll, Pitch and Yaw.
- The 'best known' parallel manipulator (see Module 4, Lecture 5).

INTRODUCTION

Modern tyre testing machine

Micro-positioning

Industrial manufacturing

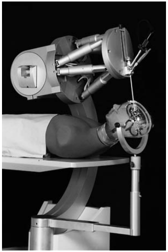

Robotic surgery

Precise alignment of mirror

Physik Instrumetente
http://www.physikinstrumente.com

Figure 26: Some modern uses of Gough-Stewart platform

Introduction

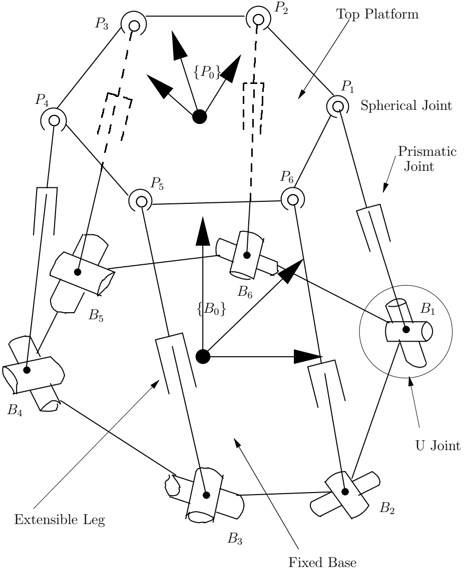

Figure 27: The Gough-Stewart platform

- Moving top platform
- Fixed base

- 6 extendable legs actuated by prismatic joints.
- Coordinated motion of 6 prismatic joints $\rightarrow$ Arbitrary 6 DOF motion of top platform

Figure 28: Motion simulation of Gough-Stewart platform

- Motion simulations done using ADAMS®.
- Click here for a video showing motion of a Gough-Stewart platfrom due to combined motion of all actuated joints.

- With actuators (P joints) locked $\rightarrow$ 0 degrees of freedom.
- Instead of actuators, strain gauge based sensors at actuator location.
- External force-moment applied at top platform can be related to *axial* forces along legs at P joint locations.
- Axial forces in legs related to strains.
- Measured strains can be related to external force-torque at top platform.

- With actuators (P joints) locked $\rightarrow$ 0 degrees of freedom.
- Instead of actuators, strain gauge based sensors at actuator location.
- External force-moment applied at top platform can be related to *axial* forces along legs at P joint locations.
- Axial forces in legs related to strains.
- Measured strains can be related to external force-torque at top platform.

- With actuators (P joints) locked $\rightarrow$ 0 degrees of freedom.
- Instead of actuators, strain gauge based sensors at actuator location.
- External force-moment applied at top platform can be related to *axial* forces along legs at P joint locations.
- Axial forces in legs related to strains.
- Measured strains can be related to external force-torque at top platform.

- With actuators (P joints) locked $\rightarrow$ 0 degrees of freedom.
- Instead of actuators, strain gauge based sensors at actuator location.
- External force-moment applied at top platform can be related to *axial* forces along legs at P joint locations.
- Axial forces in legs related to strains.
- Measured strains can be related to external force-torque at top platform.

- With actuators (P joints) locked $\rightarrow$ 0 degrees of freedom.
- Instead of actuators, strain gauge based sensors at actuator location.
- External force-moment applied at top platform can be related to *axial* forces along legs at P joint locations.
- Axial forces in legs related to strains.
- Measured strains can be related to external force-torque at top platform.

Kinematics and Statics of Gough-Stewart platform

Review

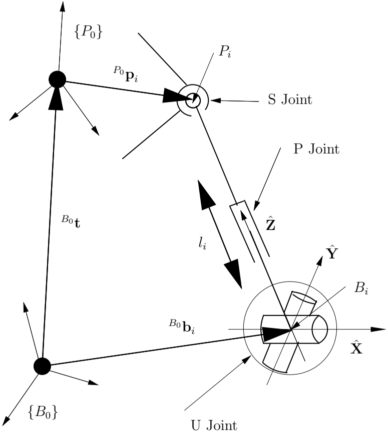

Figure 29: A leg of the Gough-Stewart platform

- Kinematics and statics (see Module 5, Lecture 5 for more details).
- Direct kinematics involve solution of a 40 degree polynomial.
- Leg vector

$$^{B_0}\mathbf{S}_i = {}^{B_0}_{P_0}[R]\,^{P_0}\mathbf{p}_i + {}^{B_0}\mathbf{t} - {}^{B_0}\mathbf{b}_i$$

- Unit vector along leg $^{B_0}\mathbf{s}_i = \frac{^{B_0}\mathbf{S}_i}{l_i}$
- Relation between external force-moment at top platform $\{Tool\}$ and leg forces f_i

$$\begin{pmatrix} ^{B_0}\mathbf{F}_{Tool} \\ --- \\ ^{B_0}\mathbf{M}_{Tool} \end{pmatrix} = \begin{bmatrix} \sum_{i=1}^{6} {}^{B_0}\mathbf{s}_i f_i \\ --- \\ \sum_{i=1}^{6} ({}^{B_0}\mathbf{b}_i \times {}^{B_0}\mathbf{s}_i) f_i \end{bmatrix}$$

REVIEW (CONTD.)

- Statics equation in matrix form

$$^{B_0}\mathscr{F}_{Tool} \triangleq \begin{pmatrix} ^{B_0}\mathbf{F}_{Tool} \\ --- \\ ^{B_0}\mathbf{M}_{Tool} \end{pmatrix} = {}^{B_0}_{Tool}[\ H\ ]\mathbf{f}$$

- The *force transformation* matrix ${}^{B_0}_{Tool}[\ H\ ]$ is given by

$$^{B_0}_{Tool}[\ H\ ] = \begin{bmatrix} ^{B_0}\mathbf{s}_1 & ^{B_0}\mathbf{s}_2 & \dots & ^{B_0}\mathbf{s}_6 \\ --- & --- & --- & --- \\ (^{B_0}\mathbf{b}_1 \times {}^{B_0}\mathbf{s}_1) & (^{B_0}\mathbf{b}_2 \times {}^{B_0}\mathbf{s}_2) & \dots & (^{B_0}\mathbf{b}_6 \times {}^{B_0}\mathbf{s}_6) \end{bmatrix}$$

where $\mathbf{f}$ is the vector of forces at the prismatic joints $(f_1, f_2, ..., f_6)^T$.
- The force transformation matrix is related to the equivalent Jacobian for the Stewart-Gough platform(see Module 5, Lecture 5).
- Leg forces can be obtained as $\mathbf{f} = {}^{B_0}_{Tool}[\ H\ ]^{-1}\,{}^{B_0}\mathscr{F}_{Tool}$

- Statics equation in matrix form

$$^{B_0}\mathscr{F}_{Tool} \triangleq \begin{pmatrix} ^{B_0}\mathbf{F}_{Tool} \\ --- \\ ^{B_0}\mathbf{M}_{Tool} \end{pmatrix} = ^{B_0}_{Tool}[\ H\ ]\mathbf{f}$$

- The *force transformation* matrix $^{B_0}_{Tool}[\ H\ ]$ is given by

$$^{B_0}_{Tool}[\ H\ ] = \begin{bmatrix} ^{B_0}\mathbf{s}_1 & ^{B_0}\mathbf{s}_2 & \dots & ^{B_0}\mathbf{s}_6 \\ --- & --- & --- & --- \\ (^{B_0}\mathbf{b}_1 \times ^{B_0}\mathbf{s}_1) & (^{B_0}\mathbf{b}_2 \times ^{B_0}\mathbf{s}_2) & \dots & (^{B_0}\mathbf{b}_6 \times ^{B_0}\mathbf{s}_6) \end{bmatrix}$$

where $\mathbf{f}$ is the vector of forces at the prismatic joints $(f_1, f_2, \dots, f_6)^T$.

- The force transformation matrix is related to the equivalent Jacobian for the Stewart-Gough platform(see Module 5, Lecture 5).
- Leg forces can be obtained as $\mathbf{f} = {^{B_0}_{Tool}[\ H\ ]}^{-1}\, ^{B_0}\mathscr{F}_{Tool}$

- Statics equation in matrix form

$$^{B_0}\mathscr{F}_{Tool} \triangleq \begin{pmatrix} ^{B_0}\mathbf{F}_{Tool} \\ --- \\ ^{B_0}\mathbf{M}_{Tool} \end{pmatrix} = {}^{B_0}_{Tool}[\ H\ ]\mathbf{f}$$

- The *force transformation* matrix ${}^{B_0}_{Tool}[\ H\ ]$ is given by

$$^{B_0}_{Tool}[\ H\ ] = \begin{bmatrix} ^{B_0}\mathbf{s}_1 & ^{B_0}\mathbf{s}_2 & \ldots & ^{B_0}\mathbf{s}_6 \\ --- & --- & --- & --- \\ (^{B_0}\mathbf{b}_1 \times {}^{B_0}\mathbf{s}_1) & (^{B_0}\mathbf{b}_2 \times {}^{B_0}\mathbf{s}_2) & \ldots & (^{B_0}\mathbf{b}_6 \times {}^{B_0}\mathbf{s}_6) \end{bmatrix}$$

  where $\mathbf{f}$ is the vector of forces at the prismatic joints $(f_1, f_2, ..., f_6)^T$.
- The force transformation matrix is related to the equivalent Jacobian for the Stewart-Gough platform(see Module 5, Lecture 5).
- Leg forces can be obtained as $\mathbf{f} = {}^{B_0}_{Tool}[\ H\ ]^{-1}\, {}^{B_0}\mathscr{F}_{Tool}$

REVIEW (CONTD.)

- Statics equation in matrix form

$$^{B_0}\mathscr{F}_{Tool} \triangleq \begin{pmatrix} ^{B_0}\mathbf{F}_{Tool} \\ --- \\ ^{B_0}\mathbf{M}_{Tool} \end{pmatrix} = {}^{B_0}_{Tool}[\ H\ ]\mathbf{f}$$

- The *force transformation* matrix $^{B_0}_{Tool}[\ H\ ]$ is given by

$$^{B_0}_{Tool}[\ H\ ] = \begin{bmatrix} ^{B_0}\mathbf{s}_1 & ^{B_0}\mathbf{s}_2 & \dots & ^{B_0}\mathbf{s}_6 \\ --- & --- & --- & --- \\ (^{B_0}\mathbf{b}_1 \times {}^{B_0}\mathbf{s}_1) & (^{B_0}\mathbf{b}_2 \times {}^{B_0}\mathbf{s}_2) & \dots & (^{B_0}\mathbf{b}_6 \times {}^{B_0}\mathbf{s}_6) \end{bmatrix}$$

where $\mathbf{f}$ is the vector of forces at the prismatic joints $(f_1, f_2, ..., f_6)^T$.

- The force transformation matrix is related to the equivalent Jacobian for the Stewart-Gough platform(see Module 5, Lecture 5).
- Leg forces can be obtained as $\mathbf{f} = {}^{B_0}_{Tool}[\ H\ ]^{-1}\, {}^{B_0}\mathscr{F}_{Tool}$

Isotropic Configurations of Gough-Stewart platform

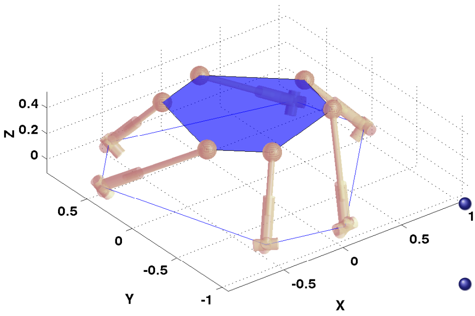

Figure 30: Gough-Stewart platform in an isotropic configuration

- Isotropic configuration $\det {}^{B_0}_{Tool}[\ H\ ] \neq 0$
- Eigenvalues of top left 3×3 and bottom right 3×3 matrix are equal (not necessary equal to each other) (see Klein and Milkos 1991, Fattah and Ghasemi 2001 and Dwarakanath et al. 2001).
- All directions are equivalent in terms of force (or moment) components.
- Isotropic configuration can be obtained in closed-form (see Bandyopadhyay & Ghosal, 2008)
- Data of Gough-Stewart platform from INRIA prototype.

Singular Configurations of Gough-Stewart platform

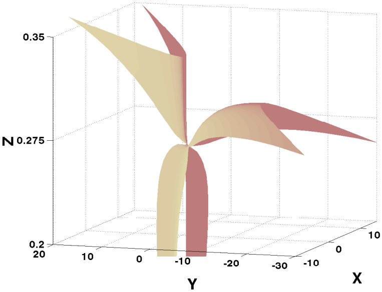

Figure 31: Singularity manifold of Gough-Stewart platform at a given orientation

- Singular configuration $\det {}^{B_0}_{Tool}[\ H\ ] = 0$
- One or more eigenvalue of ${}^{B_0}_{Tool}[\ H\ ]$ is zero!
- Gain singularity $\rightarrow$ Platform *cannot* resist one or more component of force/moment applied at the top platform.
- Singularity manifold(s) can be obtained in closed-form (see Bandyopadhyay & Ghosal, 2006)
- Position singularity manifold shown for a semi-regular Stewart platform manipulator (SRSPM) – cubic in z and a quadratic curve, but *not* an ellipse, in x and y.
- Orientation singularity manifold, at a given position, can also be obtained (see Bandyopadhyay & Ghosal, 2006).

Singular Configuration

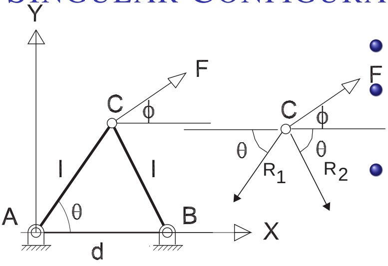

Figure 32: A planar two link hinged truss

- Planar truss with hinges.
- Force F is applied at the hinge C at an angle ϕ.
- Axial forces in the links AC and BC are

$$\begin{pmatrix} \cos\theta & -\cos\theta \\ \sin\theta & \sin\theta \end{pmatrix} \begin{pmatrix} R_1 \\ R_2 \end{pmatrix} = F \begin{pmatrix} \cos\phi \\ \sin\phi \end{pmatrix}$$

- LHS matrix is $[H]$ and for $\theta \neq 0$

$$\begin{pmatrix} R_1 \\ R_2 \end{pmatrix} = [H]^{-1} \begin{pmatrix} F\cos\phi \\ F\sin\phi \end{pmatrix} = \frac{F}{2} \begin{pmatrix} \cos\phi/\cos\theta + \sin\phi/\sin\theta \\ -\cos\phi/\cos\theta + \sin\phi/\sin\theta \end{pmatrix}$$

- For $\theta \to 0$ and $\phi \neq 0$, $R_1, R_2 \to \infty$ — F *cannot* be resisted.
- For $\theta = 0$ and $\phi \neq 0$, the eigenvalues are 1 and 0.
- Eigenvector for 0 is Y axis – F_y cannot be resisted at $\theta = 0$.
- A *small* F_y will give *large* output R_1 → *Enhanced sensitivity* or *mechanical amplification* for certain components!!

Near Singular Configuration in a Hinged Planar Truss

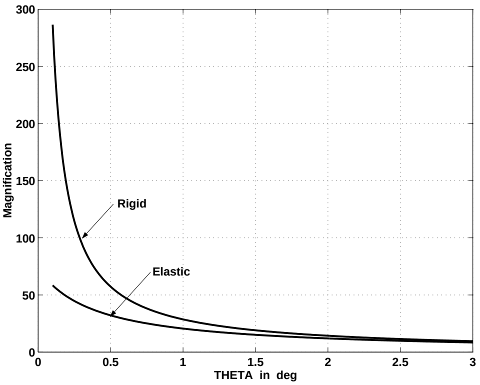

Figure 33: Force amplification Vs. θ

- For $\phi = \pi/2$, $|R_1| = |R_2| = F/(2\sin\theta)$ — θ small, $|R_1|$ and $|R_2|$ large!
- At $\theta = 1^\circ$, magnification $|R_1|/F$ is approximately 28.6.
- If AC and BC are *elastic* $\theta_{\text{new}} = \arctan(\delta + \delta_1)$ (Srinath 1983) where, $\delta = l\sin\theta$ and $\delta_1 = l\cos\theta \times (F/EA)^{1/3}$ and Poisson's ratio is 0.3.
- For elastic links $R_1 = -R_2 = F/(2\sin\theta_{new})$ – amplification/enhanced sensitivity is present but lower!!

Singular Configurations in 6×6 Gough-Stewart platform

- Force transformation $[H]$ matrix in 6×6 Gough-Stewart platform

$$ {}^{B_0}_{Tool}[\ H\ ] = \left[\begin{array}{cccc} {}^{B_0}\mathbf{s}_1 & {}^{B_0}\mathbf{s}_2 & \ldots & {}^{B_0}\mathbf{s}_6 \\ --- & --- & --- & --- \\ ({}^{B_0}\mathbf{b}_1 \times {}^{B_0}\mathbf{s}_1) & ({}^{B_0}\mathbf{b}_2 \times {}^{B_0}\mathbf{s}_2) & \ldots & ({}^{B_0}\mathbf{b}_6 \times {}^{B_0}\mathbf{s}_6) \end{array} \right] $$

- Singular configuration $\det[H] = 0$ (Merlet 1989, St-Onge and Gosselin 2000).
- Example — All legs parallel along $(0\ 0\ 1)^T$ (parallel to Z axis) and base connection points on a plane

$$ [H] = \begin{pmatrix} 0 & 0 & 0 & 0 & 0 & 0 \\ 0 & 0 & 0 & 0 & 0 & 0 \\ 1 & 1 & 1 & 1 & 1 & 1 \\ b_{1_y} & b_{2_y} & b_{3_y} & b_{4_y} & b_{5_y} & b_{6_y} \\ -b_{1_x} & -b_{2_x} & -b_{3_x} & -b_{4_x} & -b_{5_x} & -b_{6_x} \\ 0 & 0 & 0 & 0 & 0 & 0 \end{pmatrix} $$

Singular directions: $(1,0,0;0,0,0)^T$, $(0,1,0;0,0,0)^T$, and $(0,0,0;0,0,1)^T$.

- Cannot resist or *enhanced sensitivity* for F_x, F_y and M_z.

Singular Configurations in 6×6 Gough-Stewart platform

- Force transformation $[H]$ matrix in 6×6 Gough-Stewart platform

$$ {}^{B_0}_{Tool}[\ H\ ] = \left[\begin{array}{cccc} {}^{B_0}\mathbf{s}_1 & {}^{B_0}\mathbf{s}_2 & \ldots & {}^{B_0}\mathbf{s}_6 \\ --- & --- & --- & --- \\ ({}^{B_0}\mathbf{b}_1 \times {}^{B_0}\mathbf{s}_1) & ({}^{B_0}\mathbf{b}_2 \times {}^{B_0}\mathbf{s}_2) & \ldots & ({}^{B_0}\mathbf{b}_6 \times {}^{B_0}\mathbf{s}_6) \end{array} \right] $$

- Singular configuration $\det[H] = 0$ (Merlet 1989, St-Onge and Gosselin 2000).
- Example — All legs parallel along $(0\ 0\ 1)^T$ (parallel to Z axis) and base connection points on a plane

$$ [H] = \begin{pmatrix} 0 & 0 & 0 & 0 & 0 & 0 \\ 0 & 0 & 0 & 0 & 0 & 0 \\ 1 & 1 & 1 & 1 & 1 & 1 \\ b_{1_y} & b_{2_y} & b_{3_y} & b_{4_y} & b_{5_y} & b_{6_y} \\ -b_{1_x} & -b_{2_x} & -b_{3_x} & -b_{4_x} & -b_{5_x} & -b_{6_x} \\ 0 & 0 & 0 & 0 & 0 & 0 \end{pmatrix} $$

Singular directions: $(1,0,0;0,0,0)^T$, $(0,1,0;0,0,0)^T$, and $(0,0,0;0,0,1)^T$.

- Cannot resist or *enhanced sensitivity* for F_x, F_y and M_z.

Singular Configurations in 6×6 Gough-Stewart platform

- Force transformation $[H]$ matrix in 6×6 Gough-Stewart platform

$$
{}^{B_0}_{Tool}[\ H\ ] = \left[\begin{array}{cccc} {}^{B_0}\mathbf{s}_1 & {}^{B_0}\mathbf{s}_2 & \ldots & {}^{B_0}\mathbf{s}_6 \\ --- & --- & --- & --- \\ ({}^{B_0}\mathbf{b}_1 \times {}^{B_0}\mathbf{s}_1) & ({}^{B_0}\mathbf{b}_2 \times {}^{B_0}\mathbf{s}_2) & \ldots & ({}^{B_0}\mathbf{b}_6 \times {}^{B_0}\mathbf{s}_6) \end{array} \right]
$$

- Singular configuration $\det[H] = 0$ (Merlet 1989, St-Onge and Gosselin 2000).
- Example — All legs parallel along $(0\ 0\ 1)^T$ (parallel to Z axis) and base connection points on a plane

$$
[H] = \begin{pmatrix} 0 & 0 & 0 & 0 & 0 & 0 \\ 0 & 0 & 0 & 0 & 0 & 0 \\ 1 & 1 & 1 & 1 & 1 & 1 \\ b_{1_y} & b_{2_y} & b_{3_y} & b_{4_y} & b_{5_y} & b_{6_y} \\ -b_{1_x} & -b_{2_x} & -b_{3_x} & -b_{4_x} & -b_{5_x} & -b_{6_x} \\ 0 & 0 & 0 & 0 & 0 & 0 \end{pmatrix}
$$

Singular directions: $(1,0,0;0,0,0)^T$, $(0,1,0;0,0,0)^T$, and $(0,0,0;0,0,1)^T$.

- Cannot resist or *enhanced sensitivity* for F_x, F_y and M_z.

Singular Configurations in 6×6 Gough-Stewart platform

- Force transformation $[H]$ matrix in 6×6 Gough-Stewart platform

$$
{}^{B_0}_{Tool}[\ H\ ] = \left[\begin{array}{cccc} {}^{B_0}\mathbf{s}_1 & {}^{B_0}\mathbf{s}_2 & \ldots & {}^{B_0}\mathbf{s}_6 \\ --- & --- & --- & --- \\ ({}^{B_0}\mathbf{b}_1 \times {}^{B_0}\mathbf{s}_1) & ({}^{B_0}\mathbf{b}_2 \times {}^{B_0}\mathbf{s}_2) & \ldots & ({}^{B_0}\mathbf{b}_6 \times {}^{B_0}\mathbf{s}_6) \end{array} \right]
$$

- Singular configuration $\det[H] = 0$ (Merlet 1989, St-Onge and Gosselin 2000).
- Example — All legs parallel along $(0\ 0\ 1)^T$ (parallel to Z axis) and base connection points on a plane

$$
[H] = \begin{pmatrix} 0 & 0 & 0 & 0 & 0 & 0 \\ 0 & 0 & 0 & 0 & 0 & 0 \\ 1 & 1 & 1 & 1 & 1 & 1 \\ b_{1_y} & b_{2_y} & b_{3_y} & b_{4_y} & b_{5_y} & b_{6_y} \\ -b_{1_x} & -b_{2_x} & -b_{3_x} & -b_{4_x} & -b_{5_x} & -b_{6_x} \\ 0 & 0 & 0 & 0 & 0 & 0 \end{pmatrix}
$$

Singular directions: $(1,0,0;0,0,0)^T$, $(0,1,0;0,0,0)^T$, and $(0,0,0;0,0,1)^T$.

- Cannot resist or *enhanced sensitivity* for F_x, F_y and M_z.

Singular Configurations in 6×6 Gough-Stewart platform

Algorithm to obtain singular directions

- External force and leg forces are related by

$$\mathbf{F} = [H_f]\mathbf{f} = \left[\begin{array}{cccccc} \mathbf{s}_1 & \mathbf{s}_2 & \mathbf{s}_3 & \mathbf{s}_4 & \mathbf{s}_5 & \mathbf{s}_6 \end{array} \right] \mathbf{f}$$

- Maximum, minimum and intermediate values of $\mathbf{F}^T\mathbf{F}$ subject to a constraint $\mathbf{f}^T\mathbf{f} = 1$ are the eigenvalues of $[g_f] = [H_f]^T[H_f]$[4].
- Rank of $[g_f]$ is at most 3 $\Rightarrow$ 3 eigenvalues are 0 & 3 non-zero eigenvalues obtained from solution of a *cubic and in closed-form*.
- The tip of $\mathbf{F}$ lies on an ellipsoid and the axes of ellipsoid are obtained from eigenvectors corresponding to non-zero eigenvalues.
- Principal axis of ellipsoid are along principal forces.
- Directions corresponding to zero eigenvalues of $[g_f]$ are principal moments at origin.

[4]See Module 5, Lecture 2 for a similar treatment for velocities.

SINGULAR CONFIGURATIONS IN 6×6 GOUGH-STEWART PLATFORM

ALGORITHM TO OBTAIN SINGULAR DIRECTIONS

- External force and leg forces are related by

$$\mathbf{F} = [H_f]\mathbf{f} = \begin{bmatrix} \mathbf{s}_1 & \mathbf{s}_2 & \mathbf{s}_3 & \mathbf{s}_4 & \mathbf{s}_5 & \mathbf{s}_6 \end{bmatrix} \mathbf{f}$$

- Maximum, minimum and intermediate values of $\mathbf{F}^T\mathbf{F}$ subject to a constraint $\mathbf{f}^T\mathbf{f} = 1$ are the eigenvalues of $[g_f] = [H_f]^T[H_f]$[4].
- Rank of $[g_f]$ is at most 3 $\Rightarrow$ 3 eigenvalues are 0 & 3 non-zero eigenvalues obtained from solution of a *cubic and in closed-form*.
- The tip of $\mathbf{F}$ lies on an ellipsoid and the axes of ellipsoid are obtained from eigenvectors corresponding to non-zero eigenvalues.
- Principal axis of ellipsoid are along principal forces.
- Directions corresponding to zero eigenvalues of $[g_f]$ are principal moments at origin.

[4] See Module 5, Lecture 2 for a similar treatment for velocities.

Singular Configurations in 6×6 Gough-Stewart platform

Algorithm to obtain singular directions

- External force and leg forces are related by

$$\mathbf{F} = [H_f]\mathbf{f} = \begin{bmatrix} \mathbf{s}_1 & \mathbf{s}_2 & \mathbf{s}_3 & \mathbf{s}_4 & \mathbf{s}_5 & \mathbf{s}_6 \end{bmatrix} \mathbf{f}$$

- Maximum, minimum and intermediate values of $\mathbf{F}^T\mathbf{F}$ subject to a constraint $\mathbf{f}^T\mathbf{f} = 1$ are the eigenvalues of $[g_f] = [H_f]^T[H_f]$[4].
- Rank of $[g_f]$ is at most 3 $\Rightarrow$ 3 eigenvalues are 0 & 3 non-zero eigenvalues obtained from solution of a *cubic and in closed-form*.
- The tip of $\mathbf{F}$ lies on an ellipsoid and the axes of ellipsoid are obtained from eigenvectors corresponding to non-zero eigenvalues.
- Principal axis of ellipsoid are along principal forces.
- Directions corresponding to zero eigenvalues of $[g_f]$ are principal moments at origin.

[4]See Module 5, Lecture 2 for a similar treatment for velocities.

Singular Configurations in 6×6 Gough-Stewart platform

Algorithm to obtain singular directions

- External force and leg forces are related by

$$\mathbf{F} = [H_f]\mathbf{f} = \begin{bmatrix} \mathbf{s}_1 & \mathbf{s}_2 & \mathbf{s}_3 & \mathbf{s}_4 & \mathbf{s}_5 & \mathbf{s}_6 \end{bmatrix} \mathbf{f}$$

- Maximum, minimum and intermediate values of $\mathbf{F}^T\mathbf{F}$ subject to a constraint $\mathbf{f}^T\mathbf{f} = 1$ are the eigenvalues of $[g_f] = [H_f]^T[H_f]$[4].
- Rank of $[g_f]$ is at most 3 $\Rightarrow$ 3 eigenvalues are 0 & 3 non-zero eigenvalues obtained from solution of a *cubic and in closed-form*.
- The tip of $\mathbf{F}$ lies on an ellipsoid and the axes of ellipsoid are obtained from eigenvectors corresponding to non-zero eigenvalues.
- Principal axis of ellipsoid are along principal forces.
- Directions corresponding to zero eigenvalues of $[g_f]$ are principal moments at origin.

[4]See Module 5, Lecture 2 for a similar treatment for velocities.

Singular Configurations in 6×6 Gough-Stewart platform

Algorithm to obtain singular directions

- External force and leg forces are related by

$$\mathbf{F} = [H_f]\mathbf{f} = \left[\begin{array}{cccccc} \mathbf{s}_1 & \mathbf{s}_2 & \mathbf{s}_3 & \mathbf{s}_4 & \mathbf{s}_5 & \mathbf{s}_6 \end{array} \right] \mathbf{f}$$

- Maximum, minimum and intermediate values of $\mathbf{F}^T\mathbf{F}$ subject to a constraint $\mathbf{f}^T\mathbf{f} = 1$ are the eigenvalues of $[g_f] = [H_f]^T[H_f]$[4].
- Rank of $[g_f]$ is at most 3 $\Rightarrow$ 3 eigenvalues are 0 & 3 non-zero eigenvalues obtained from solution of a *cubic and in closed-form*.
- The tip of $\mathbf{F}$ lies on an ellipsoid and the axes of ellipsoid are obtained from eigenvectors corresponding to non-zero eigenvalues.
- Principal axis of ellipsoid are along principal forces.
- Directions corresponding to zero eigenvalues of $[g_f]$ are principal moments at origin.

[4] See Module 5, Lecture 2 for a similar treatment for velocities.

Singular Configurations in 6×6 Gough-Stewart platform

Algorithm to obtain singular directions

- External force and leg forces are related by

$$\mathbf{F} = [H_f]\mathbf{f} = \begin{bmatrix} \mathbf{s}_1 & \mathbf{s}_2 & \mathbf{s}_3 & \mathbf{s}_4 & \mathbf{s}_5 & \mathbf{s}_6 \end{bmatrix} \mathbf{f}$$

- Maximum, minimum and intermediate values of $\mathbf{F}^T\mathbf{F}$ subject to a constraint $\mathbf{f}^T\mathbf{f} = 1$ are the eigenvalues of $[g_f] = [H_f]^T[H_f]$[4].
- Rank of $[g_f]$ is at most 3 $\Rightarrow$ 3 eigenvalues are 0 & 3 non-zero eigenvalues obtained from solution of a *cubic and in closed-form*.
- The tip of $\mathbf{F}$ lies on an ellipsoid and the axes of ellipsoid are obtained from eigenvectors corresponding to non-zero eigenvalues.
- Principal axis of ellipsoid are along principal forces.
- Directions corresponding to zero eigenvalues of $[g_f]$ are principal moments at origin.

[4] See Module 5, Lecture 2 for a similar treatment for velocities.

Singular Configurations in 6×6 Gough-Stewart platform

- Eigenvector of $[g_f]$ mapped by $[H]$ are

$$[H][X] = \left(\begin{array}{c|c} [0] & [F]^* \\ --- & --- \\ [M]_O{}^* & [M]_p{}^* \end{array} \right)$$

  $[F]^*$ is a 3×3 matrix of principal forces, $[M]_O{}^*$ is a 3×3 matrix of principal moments at the origin, and $[M]_p{}^*$ is a 3×3 matrix of principal moments at centre of platform.

- Rank of $[g_f]$ less than 3 $\Rightarrow$ Singularity in force domain.
- Eigenvectors of $[g_f]$, corresponding to zero eigenvalue, mapped by $[H]$ give direction(s) where force cannot be resisted — same as null space $[F]^*$.
- Singular directions of moment — Null space of $[M]_O{}^*$.

Singular Configurations in 6×6 Gough-Stewart platform

- Eigenvector of $[g_f]$ mapped by $[H]$ are

$$[H][X] = \left(\begin{array}{c|c} [0] & [F]^* \\ --- & --- \\ [M]_O{}^* & [M]_p{}^* \end{array} \right)$$

  $[F]^*$ is a 3×3 matrix of principal forces, $[M]_O{}^*$ is a 3×3 matrix of principal moments at the origin, and $[M]_p{}^*$ is a 3×3 matrix of principal moments at centre of platform.

- Rank of $[g_f]$ less than 3 $\Rightarrow$ Singularity in force domain.
- Eigenvectors of $[g_f]$, corresponding to zero eigenvalue, mapped by $[H]$ give direction(s) where force cannot be resisted — same as null space $[F]^*$.
- Singular directions of moment — Null space of $[M]_O{}^*$.

Singular Configurations in 6×6 Gough-Stewart platform

- Eigenvector of $[g_f]$ mapped by $[H]$ are

$$[H][X] = \left(\begin{array}{c|c} [0] & [F]^* \\ --- & --- \\ [M]_O{}^* & [M]_p{}^* \end{array} \right)$$

  $[F]^*$ is a 3×3 matrix of principal forces, $[M]_O{}^*$ is a 3×3 matrix of principal moments at the origin, and $[M]_p{}^*$ is a 3×3 matrix of principal moments at centre of platform.

- Rank of $[g_f]$ less than 3 $\Rightarrow$ Singularity in force domain.
- Eigenvectors of $[g_f]$, corresponding to zero eigenvalue, mapped by $[H]$ give direction(s) where force cannot be resisted — same as null space $[F]^*$.
- Singular directions of moment — Null space of $[M]_O{}^*$.

Singular Configurations in 6×6 Gough-Stewart platform

- Eigenvector of $[g_f]$ mapped by $[H]$ are

$$[H][X] = \left(\begin{array}{c|c} [0] & [F]^* \\ --- & --- \\ {[M]_O}^* & {[M]_p}^* \end{array} \right)$$

  $[F]^*$ is a 3×3 matrix of principal forces, ${[M]_O}^*$ is a 3×3 matrix of principal moments at the origin, and ${[M]_p}^*$ is a 3×3 matrix of principal moments at centre of platform.

- Rank of $[g_f]$ less than 3 $\Rightarrow$ Singularity in force domain.
- Eigenvectors of $[g_f]$, corresponding to zero eigenvalue, mapped by $[H]$ give direction(s) where force cannot be resisted — same as null space $[F]^*$.
- Singular directions of moment — Null space of ${[M]_O}^*$.

Algorithm to obtain singular directions in Gough-Stewart platform

- Enumerate all possible $6-6$ Gough-Stewart platforms by choosing pairs of base and platform points. For each of the configurations,
  - Compute the number of zero eigenvalues of $[H]$. This will give the total number of singular directions *including* force and moments.
  - Obtain all eigenvalues and corresponding eigenvectors *symbolically* for $[g_f]$ using a symbolic manipulation package.
  - Obtain the matrix $[H][X]$ and sub-matrices $[F]^*$ and $[M]^*_O$ (see previous slide).
  - Obtain null space vectors of $[F]^*$ and $[M]^*_O$ to obtain the singular force and moment directions (if any).
- Eigenvalues and eigenvectors can be obtained *symbolically* $\rightarrow$ Singular directions can be obtained symbolically.
- Singular directions obtained using Mathematica®(Wolfram 2004).

Algorithm to obtain singular directions in Gough-Stewart platform

- Enumerate all possible $6-6$ Gough-Stewart platforms by choosing pairs of base and platform points. For each of the configurations,
  - Compute the number of zero eigenvalues of $[H]$. This will give the total number of singular directions *including* force and moments.
  - Obtain all eigenvalues and corresponding eigenvectors *symbolically* for $[g_f]$ using a symbolic manipulation package.
  - Obtain the matrix $[H][X]$ and sub-matrices $[F]^*$ and $[M]^*_O$ (see previous slide).
  - Obtain null space vectors of $[F]^*$ and $[M]^*_O$ to obtain the singular force and moment directions (if any).
- Eigenvalues and eigenvectors can be obtained *symbolically* $\rightarrow$ Singular directions can be obtained symbolically.
- Singular directions obtained using Mathematica®(Wolfram 2004).

Algorithm to obtain singular directions in Gough-Stewart platform

- Enumerate all possible $6-6$ Gough-Stewart platforms by choosing pairs of base and platform points. For each of the configurations,
  - Compute the number of zero eigenvalues of $[H]$. This will give the total number of singular directions *including* force and moments.
  - Obtain all eigenvalues and corresponding eigenvectors *symbolically* for $[g_f]$ using a symbolic manipulation package.
  - Obtain the matrix $[H][X]$ and sub-matrices $[F]^*$ and $[M]^*_O$ (see previous slide).
  - Obtain null space vectors of $[F]^*$ and $[M]^*_O$ to obtain the singular force and moment directions (if any).
- Eigenvalues and eigenvectors can be obtained *symbolically* $\rightarrow$ Singular directions can be obtained symbolically.
- Singular directions obtained using Mathematica®(Wolfram 2004).

Examples of Singular Directions in 6×6 Gough-Stewart platform

Table 1: Examples of Singular Directions in 6×6 Gough-Stewart platform configurations

	Leg Connections						$*$	Singular
	Leg 1	Leg 2	Leg 3	Leg 4	Leg 5	Leg 6		Directions
1	$B_1 - P_1$	$B_2 - P_2$	$B_3 - P_3$	$B_4 - P_4$	$B_5 - P_5$	$B_6 - P_6$	3	F_x, F_y, M_z
2	$B_1 - P_2$	$B_2 - P_1$	$B_3 - P_3$	$B_4 - P_4$	$B_5 - P_5$	$B_6 - P_6$	2	F_x, M_z
3	$B_1 - P_2$	$B_2 - P_1$	$B_3 - P_4$	$B_4 - P_3$	$B_5 - P_5$	$B_6 - P_6$	1	M_z
4	$B_1 - P_2$	$B_2 - P_1$	$B_3 - P_4$	$B_4 - P_3$	$B_5 - P_6$	$B_6 - P_5$	0	none
5	$B_1 - P_1$	$B_2 - P_3$	$B_3 - P_2$	$B_4 - P_5$	$B_5 - P_4$	$B_6 - P_6$	1	M_z
6	$B_1 - P_1$	$B_2 - P_6$	$B_3 - P_5$	$B_4 - P_4$	$B_5 - P_3$	$B_6 - P_2$	2	F_x, M_z
7	$B_1 - P_1$	$B_2 - P_3$	$B_3 - P_2$	$B_4 - P_4$	$B_5 - P_6$	$B_6 - P_5$	1	F_y
8	$B_1 - P_2$	$B_2 - P_3$	$B_3 - P_4$	$B_4 - P_5$	$B_5 - P_6$	$B_6 - P_1$	3	M_x, M_y, M_z

$*$ – Column indicate number of zero eigenvalues of $[H]$.

- B_i, P_i, $i = 1, \ldots 6$ are Base and Platform connection points.

Near Singular Configuration in 6×6 Gough-Stewart platform

- Configuration 1 chosen for sensor developement — *Enhanced sensitivity* for F_x, F_y and M_z.
- Both top and bottom platform are regular hexagons of equal sides.
- At *exactly* singular configuration, legs are *exactly* vertical and amplification is infinite — Not desirable!
- Gough-Stewart platform, Configuration # 1, at a *near* singularity
  - The legs are *not exactly* vertical.
  - Top and bottom platform not *aligned* and included half-angle changed from 30° to 33° $\rightarrow$ Top platform rotated by 3°!
  - det $[H] \neq 0 \rightarrow$ *Near singular* with condition number of $[H]$ about 1900.
  - Amplification of about 10 (and not infinity)!

Near Singular Configuration in 6×6 Gough-Stewart platform

- Configuration 1 chosen for sensor developement — *Enhanced sensitivity* for F_x, F_y and M_z.
- Both top and bottom platform are regular hexagons of equal sides.
- At *exactly* singular configuration, legs are *exactly* vertical and amplification is infinite — Not desirable!
- Gough-Stewart platform, Configuration # 1, at a *near* singularity
  - The legs are *not exactly* vertical.
  - Top and bottom platform not *aligned* and included half-angle changed from 30° to 33° $\rightarrow$ Top platform rotated by 3°!
  - det $[H] \neq 0 \rightarrow$ *Near singular* with condition number of $[H]$ about 1900.
  - Amplification of about 10 (and not infinity)!

Near Singular Configuration in 6×6 Gough-Stewart platform

- Configuration 1 chosen for sensor developement — *Enhanced sensitivity* for F_x, F_y and M_z.
- Both top and bottom platform are regular hexagons of equal sides.
- At *exactly* singular configuration, legs are *exactly* vertical and amplification is infinite — Not desirable!
- Gough-Stewart platform, Configuration # 1, at a *near* singularity
  - The legs are *not exactly* vertical.
  - Top and bottom platform not *aligned* and included half-angle changed from 30° to 33° $\rightarrow$ Top platform rotated by 3°!
  - det $[H] \neq 0 \rightarrow$ *Near singular* with condition number of $[H]$ about 1900.
  - Amplification of about 10 (and not infinity)!

Near Singular Configuration in 6×6 Gough-Stewart platform

- Configuration 1 chosen for sensor developement — *Enhanced sensitivity* for F_x, F_y and M_z.
- Both top and bottom platform are regular hexagons of equal sides.
- At *exactly* singular configuration, legs are *exactly* vertical and amplification is infinite — Not desirable!
- Gough-Stewart platform, Configuration # 1, at a *near* singularity
  - The legs are *not exactly* vertical.
  - Top and bottom platform not *aligned* and included half-angle changed from 30° to 33° $\rightarrow$ Top platform rotated by 3°!
  - det $[H] \neq 0 \rightarrow$ *Near singular* with condition number of $[H]$ about 1900.
  - Amplification of about 10 (and not infinity)!

Table 2: Nominal geometry of 6-6 Stewart Platform with $\gamma = 33^\circ$

Base coordinates				Platform coordinates			
Point No.	x mm	y mm	z mm	Point No	X mm	Y mm	Z mm
b_1	43.30	25.0	0.0	p_1	41.93	27.23	100
b_2	0	50.0	0.0	p_2	2.616	49.93	100
b_3	-43.30	25.0	0.0	p_3	-44.55	22.70	100
b_4	-43.30	-25.0	0.0	p_4	-44.55	-22.70	100
b_5	0	-50	0.0	p_5	2.616	-49.93	100
b_6	43.3	-25.0	0.0	p_6	41.93	-27.23	100

- Expected to give enhanced sensitivity to F_x, F_y and M_z.
- Near singular configuration – can invert $[H]$ if and when required.

Gough-Stewart Platform based Sensor

Flexible Hinges

- Kinematic joints (S or U) give rise to unpredictable friction!
- Flexible hinges (Paros and Weisboard 1965, Zhang and Fasse 2001) much better – No friction! (see also McInroy and Hamann 2000).

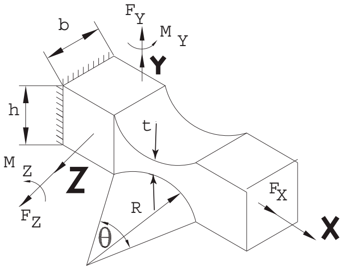

Figure 34: Flexure hinges – rectangular cross-section

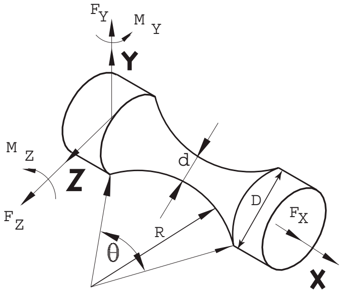

Figure 35: Flexure hinges – circular cross-section

- Geometry (t, R, θ) or (d, D, θ) can be designed to give required lateral and longitudinal stiffness (or compliance).
- For small motion (sensor) good approximation to kinematic joints.

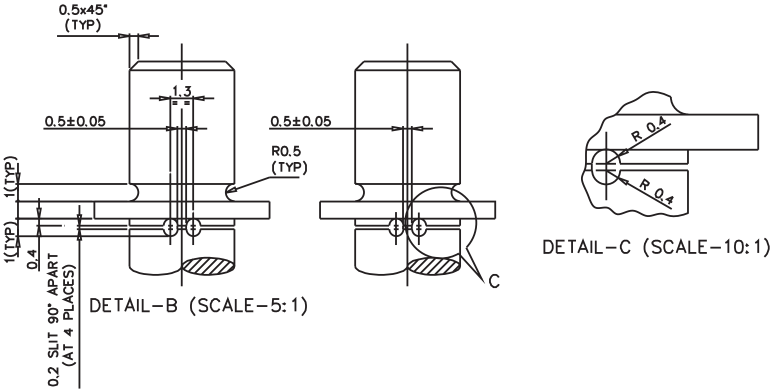

Figure 36: Detailed view of flexure hinges

- Hinges (also leg and ring): Titanium alloy of yield strength 880 N $/\mathrm{mm}^2$.
- No rotation permitted beyond 3.8° to prevent failure!

Gough-Stewart Platform based Sensor

Sensing Element

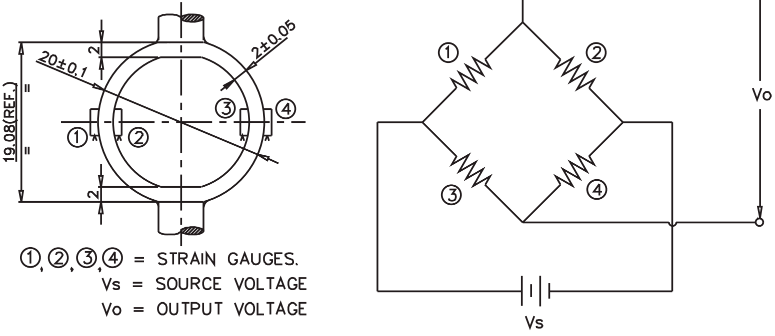

Figure 37: Schematic of ring shaped sensing element

- Ring shaped sensing element from Titanium alloy rod.
- Ring mid-plane has largest stress (and strain) when axial load applied.
- For 30 N axial compressive load, 145 micro-strains (compressive)at inside surface and 110 micro-strains (tensile) at the outside surface — 510 micro-strains in full bridge configuration.

Finite Element Analysis

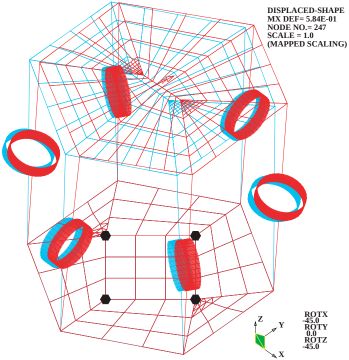

Figure 38: Deflection (mm) of sensor

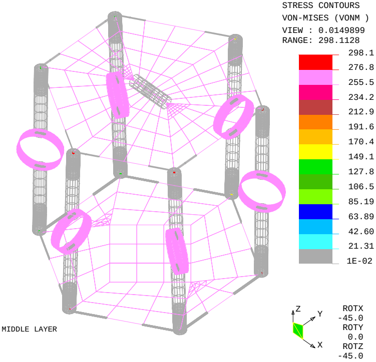

Figure 39: Stress ($\mathrm{N/mm^2}$) in sensor

- Finite element model (in NISA (1997)) of top and bottom platform and six legs with hinges and sensing element created.
- Applied loading of $F_x = F_y = F_z = 0.98$ N, $M_x = M_y = M_z = 49.05$
- Maximum deflection 0.5 mm and maximum stress about 294 $\mathrm{N/mm^2}$ at the flexible hinges — Safe design!

Gough-Stewart Platform based Sensor

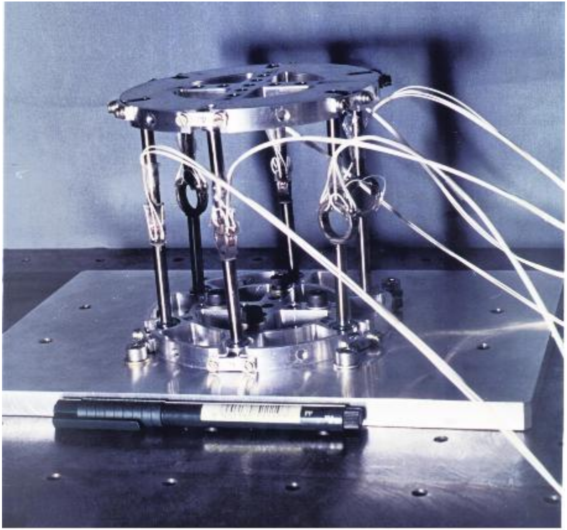

Figure 40: Prototype Gough-Stewart platform based force-torque sensor

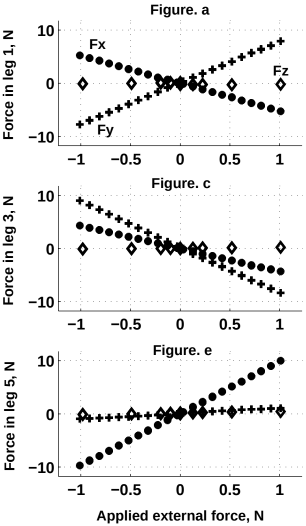

Figure 41: Experimental data for external applied force

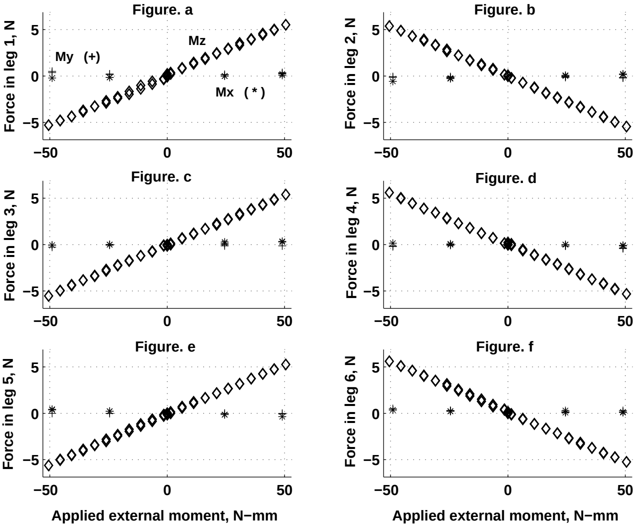

Figure 42: Experimental data for external applied moment

- Calibration of leg – Measure strain in legs for known loading.
- Obtain calibration constant μ−strain /N for each leg.
  - Leg 1 – 13.786, Leg 2 – 13.958, Leg 3 – 14.102
  - Leg 4 – 13.921, Leg 5 – 13.994, leg 6 – 14.046
- Convert measured strains to leg forces f_i, $i = 1, ..., 6$ for applied loads.
- Obtain elements of $[H]$ matrix from experimental data
  - From $(\mathbf{F}; \mathbf{M})^T = [H]\mathbf{f}$, write

$$F_x = f_1 H_{11} + f_2 H_{12} + f_3 H_{13} + f_4 H_{14} + f_5 H_{15} + f_6 H_{16}$$

    f_i measured leg forces, H_{1j} unknown elements of first row of $[H]$.
  - From n sets of measurements f_i, $i = 1, ..., 6$, form $n \times 6$ matrix $[f]$.
  - The elements H_{1j} are

$$(H_{1j}, H_{2j}, H_{3j}, H_{4j}, H_{5j}, H_{6j})^T = [f]^{\#}(F_{1x}, F_{2x}, ..., F_{nx})^T$$

    where $[f]^{\#}$ is the *pseudo-inverse* of $[f]$.
  - Find other rows of $[H]$ in similar manner.

- Calibration of leg – Measure strain in legs for known loading.
- Obtain calibration constant $\mu-$strain /N for each leg.
  - Leg 1 – 13.786, Leg 2 – 13.958, Leg 3 – 14.102
  - Leg 4 – 13.921, Leg 5 – 13.994, leg 6 – 14.046
- Convert measured strains to leg forces f_i, $i = 1,...,6$ for applied loads.
- Obtain elements of $[H]$ matrix from experimental data
  - From $(\mathbf{F};\mathbf{M})^T = [H]\mathbf{f}$, write

$$F_x = f_1 H_{11} + f_2 H_{12} + f_3 H_{13} + f_4 H_{14} + f_5 H_{15} + f_6 H_{16}$$

    f_i measured leg forces, H_{1j} unknown elements of first row of $[H]$.
  - From n sets of measurements f_i, $i = 1,...,6$, form $n \times 6$ matrix $[f]$.
  - The elements H_{1j} are

$$(H_{1j}, H_{2j}, H_{3j}, H_{4j}, H_{5j}, H_{6j})^T = [f]^{\#}(F_{1x}, F_{2x}, ..., F_{nx})^T$$

    where $[f]^{\#}$ is the *pseudo-inverse* of $[f]$.
  - Find other rows of $[H]$ in similar manner.

- Calibration of leg – Measure strain in legs for known loading.
- Obtain calibration constant $\mu-$strain /N for each leg.
    - Leg 1 – 13.786, Leg 2 – 13.958, Leg 3 – 14.102
    - Leg 4 – 13.921, Leg 5 – 13.994, leg 6 – 14.046
- Convert measured strains to leg forces $f_i,\ i = 1, ..., 6$ for applied loads.
- Obtain elements of $[H]$ matrix from experimental data
    - From $(\mathbf{F}; \mathbf{M})^T = [H]\mathbf{f}$, write

$$F_x = f_1 H_{11} + f_2 H_{12} + f_3 H_{13} + f_4 H_{14} + f_5 H_{15} + f_6 H_{16}$$

      f_i measured leg forces, H_{1j} unknown elements of first row of $[H]$.
    - From n sets of measurements $f_i,\ i = 1, ..., 6$, form $n \times 6$ matrix $[f]$.
    - The elements H_{1j} are

$$(H_{1j}, H_{2j}, H_{3j}, H_{4j}, H_{5j}, H_{6j})^T = [f]^{\#}(F_{1x}, F_{2x}, ..., F_{nx})^T$$

      where $[f]^{\#}$ is the *pseudo-inverse* of $[f]$.
    - Find other rows of $[H]$ in similar manner.

- Calibration of leg – Measure strain in legs for known loading.
- Obtain calibration constant $\mu-$strain /N for each leg.
  - Leg 1 – 13.786, Leg 2 – 13.958, Leg 3 – 14.102
  - Leg 4 – 13.921, Leg 5 – 13.994, leg 6 – 14.046
- Convert measured strains to leg forces f_i, $i = 1, ..., 6$ for applied loads.
- Obtain elements of $[H]$ matrix from experimental data
  - From $(\mathbf{F}; \mathbf{M})^T = [H]\mathbf{f}$, write

$$F_x = f_1 H_{11} + f_2 H_{12} + f_3 H_{13} + f_4 H_{14} + f_5 H_{15} + f_6 H_{16}$$

    f_i measured leg forces, H_{1j} unknown elements of first row of $[H]$.
  - From n sets of measurements f_i, $i = 1, ..., 6$, form $n \times 6$ matrix $[f]$.
  - The elements H_{1j} are

$$(H_{1j}, H_{2j}, H_{3j}, H_{4j}, H_{5j}, H_{6j})^T = [f]^{\#}(F_{1x}, F_{2x}, ..., F_{nx})^T$$

    where $[f]^{\#}$ is the *pseudo-inverse* of $[f]$.
  - Find other rows of $[H]$ in similar manner.

- Calibration $[H_c]$ matrix is obtained as

$$[H_c] = \begin{bmatrix} -0.0195 & 0.0279 & -0.0266 & -0.0223 & 0.0369 & -0.0117 \\ 0.0287 & -0.0076 & -0.0368 & 0.0280 & 0.0036 & -0.0272 \\ 0.8890 & 0.8294 & 0.8321 & 0.8845 & 0.9704 & 0.9712 \\ 22.7237 & 44.3631 & 21.0266 & -18.6015 & -45.1386 & -26.4990 \\ -6.7289 & -5.5169 & -5.0906 & -4.8826 & -5.1129 & -6.4894 \\ 1.3319 & -1.5084 & 1.8969 & -1.4110 & 1.2823 & -1.9917 \end{bmatrix}$$

- Condition No. is 1351 compared to a computed 1910.
- Obtain *unknown* $(\mathbf{F};\mathbf{M})^T$ from $[H_c]\mathbf{f}$, where $\mathbf{f}$ is measured leg forces.

Gough-Stewart Platform based Sensor
Calibration (contd.)

- Calibration $[H_c]$ matrix is obtained as

$$[H_c] = \begin{bmatrix} -0.0195 & 0.0279 & -0.0266 & -0.0223 & 0.0369 & -0.0117 \\ 0.0287 & -0.0076 & -0.0368 & 0.0280 & 0.0036 & -0.0272 \\ 0.8890 & 0.8294 & 0.8321 & 0.8845 & 0.9704 & 0.9712 \\ 22.7237 & 44.3631 & 21.0266 & -18.6015 & -45.1386 & -26.4990 \\ -6.7289 & -5.5169 & -5.0906 & -4.8826 & -5.1129 & -6.4894 \\ 1.3319 & -1.5084 & 1.8969 & -1.4110 & 1.2823 & -1.9917 \end{bmatrix}$$

- Condition No. is 1351 compared to a computed 1910.
- Obtain *unknown* $(\mathbf{F};\mathbf{M})^T$ from $[H_c]\mathbf{f}$, where $\mathbf{f}$ is measured leg forces.

GOUGH-STEWART PLATFORM BASED SENSOR

CALIBRATION (CONTD.)

- Calibration $[H_c]$ matrix is obtained as

$$[H_c] = \begin{bmatrix} -0.0195 & 0.0279 & -0.0266 & -0.0223 & 0.0369 & -0.0117 \\ 0.0287 & -0.0076 & -0.0368 & 0.0280 & 0.0036 & -0.0272 \\ 0.8890 & 0.8294 & 0.8321 & 0.8845 & 0.9704 & 0.9712 \\ 22.7237 & 44.3631 & 21.0266 & -18.6015 & -45.1386 & -26.4990 \\ -6.7289 & -5.5169 & -5.0906 & -4.8826 & -5.1129 & -6.4894 \\ 1.3319 & -1.5084 & 1.8969 & -1.4110 & 1.2823 & -1.9917 \end{bmatrix}$$

- Condition No. is 1351 compared to a computed 1910.
- Obtain *unknown* $(\mathbf{F};\mathbf{M})^T$ from $[H_c]\mathbf{f}$, where $\mathbf{f}$ is measured leg forces.

- For a combined 3D external loading of $(0.9123, 0.9123, 0)^T$ N force and $(-10.0356, 10.03560, 0)^T$ N-mm moment, the measured values of forces and moments are $(0.9270, 0.8819, 0.0265)^T$ N and $(-13.0081, 10.1789, -1.4352)^T$ N-mm respectively. It may be noted that the FEA computed values for the externally applied 3D loading are $(0.9241, 0.8809, 0.0932)^T$ N of force and $(-19.2041, 12.3772, -0.5258)^T$ N-mm.
- For a combined 3D loading of $(0.9123, 0.9123, 0)^T$ N force and $(-10.0356, 10.0356, -45.6165)^T$ N-mm moment, the measured values of forces and moments are $(0.8937, 0.9153, 0.1462)^T$ N and $(-12.2085, 8.9987, -45.9569)^T$ N-mm respectively. The computed FEA values for the 3D loading is $(0.8780, 0.9261, 0.2688)^T$ N force and $(-21.8783, 18.0896, -43.7448)^T$ N-mm moment.

Gough-Stewart Platform based Sensor

- The performance of the prototype sensor is very good for sensing forces and moments in the chosen sensitive directions and errors are around 3%.
- A magnification of about 10 is observed in the sensitive directions.
- The performance of the prototype sensor in the non-sensitive directions is less accurate — More electronic amplification is required.
- The computed FEA values are in general larger. This is expected since FE based models are known to be stiffer.

Gough-Stewart Platform based Sensor

Moment Sensitive Configuration

- Configuration # 8 is sensitive to moments.
- The connection sequence is $B_1 - P_2,\ B_2 - P_3\ \ldots\ B_6 - P_1$

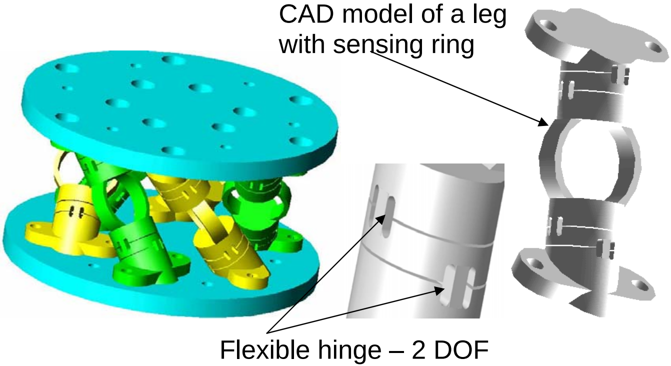

Figure 43: CAD model of sensor sensitive to moment components

Gough-Stewart Platform based Sensor

Moment Sensitive Configuration

Figure 44: Prototype sensor sensitive to moment components

- Testing under progress.

Summary

- Gough-Stewart as a six component force-torque sensor.
- Isotropic and singular configurations.
- Algorithm to obtain singular directions – can be done symbolically!
- Design of a 6 component force-torque sensor sensitive to F_x, F_y and M_z.
  - Kinematic design – choice of configuration and geometry.
  - Design of flexible hinges and sensing element.
  - Finite element analysis of full sensor.
  - Prototyping, calibration and testing.
- Sensor sensitive to moments.
- Can design a *class* of Gough-Stewart platform based sensors with desired (enhanced) sensitivities!!

SUMMARY

- Gough-Stewart as a six component force-torque sensor.
- Isotropic and singular configurations.
- Algorithm to obtain singular directions – can be done symbolically!
- Design of a 6 component force-torque sensor sensitive to F_x, F_y and M_z.
  - Kinematic design – choice of configuration and geometry.
  - Design of flexible hinges and sensing element.
  - Finite element analysis of full sensor.
  - Prototyping, calibration and testing.
- Sensor sensitive to moments.
- Can design a *class* of Gough-Stewart platform based sensors with desired (enhanced) sensitivities!!

SUMMARY

- Gough-Stewart as a six component force-torque sensor.
- Isotropic and singular configurations.
- Algorithm to obtain singular directions – can be done symbolically!
- Design of a 6 component force-torque sensor sensitive to F_x, F_y and M_z.
  - Kinematic design – choice of configuration and geometry.
  - Design of flexible hinges and sensing element.
  - Finite element analysis of full sensor.
  - Prototyping, calibration and testing.
- Sensor sensitive to moments.
- Can design a *class* of Gough-Stewart platform based sensors with desired (enhanced) sensitivities!!

SUMMARY

- Gough-Stewart as a six component force-torque sensor.
- Isotropic and singular configurations.
- Algorithm to obtain singular directions – can be done symbolically!
- Design of a 6 component force-torque sensor sensitive to F_x, F_y and M_z.
  - Kinematic design – choice of configuration and geometry.
  - Design of flexible hinges and sensing element.
  - Finite element analysis of full sensor.
  - Prototyping, calibration and testing.
- Sensor sensitive to moments.
- Can design a *class* of Gough-Stewart platform based sensors with desired (enhanced) sensitivities!!

Summary

- Gough-Stewart as a six component force-torque sensor.
- Isotropic and singular configurations.
- Algorithm to obtain singular directions – can be done symbolically!
- Design of a 6 component force-torque sensor sensitive to F_x, F_y and M_z.
  - Kinematic design – choice of configuration and geometry.
  - Design of flexible hinges and sensing element.
  - Finite element analysis of full sensor.
  - Prototyping, calibration and testing.
- Sensor sensitive to moments.
- Can design a *class* of Gough-Stewart platform based sensors with desired (enhanced) sensitivities!!

SUMMARY

- Gough-Stewart as a six component force-torque sensor.
- Isotropic and singular configurations.
- Algorithm to obtain singular directions – can be done symbolically!
- Design of a 6 component force-torque sensor sensitive to F_x, F_y and M_z.
    - Kinematic design – choice of configuration and geometry.
    - Design of flexible hinges and sensing element.
    - Finite element analysis of full sensor.
    - Prototyping, calibration and testing.
- Sensor sensitive to moments.
- Can design a *class* of Gough-Stewart platform based sensors with desired (enhanced) sensitivities!!

OUTLINE

Contents of Lecture[5]

- Introduction
- Over-constrained mechanisms and deployable structures.
- Constraint Jacobian and obtaining redundant links and joints.
- Kinematics of SLE based deployable structures.
- Statics of SLE based deployable structures.
- Summary

[5]This Lecture is based on material from Nagaraj (2009) and Nagaraj et al. (2009, 2010). Please see these and reference listed at the end for more details.

CONTENTS OF LECTURE[5]

- Introduction
- Over-constrained mechanisms and deployable structures.
- Constraint Jacobian and obtaining redundant links and joints.
- Kinematics of SLE based deployable structures.
- Statics of SLE based deployable structures.
- Summary

[5] This Lecture is based on material from Nagaraj (2009) and Nagaraj et al. (2009, 2010). Please see these and reference listed at the end for more details.

CONTENTS OF LECTURE[5]

- Introduction
- Over-constrained mechanisms and deployable structures.
- Constraint Jacobian and obtaining redundant links and joints.
- Kinematics of SLE based deployable structures.
- Statics of SLE based deployable structures.
- Summary

[5]This Lecture is based on material from Nagaraj (2009) and Nagaraj et al. (2009, 2010). Please see these and reference listed at the end for more details.

Contents of Lecture[5]

- Introduction
- Over-constrained mechanisms and deployable structures.
- Constraint Jacobian and obtaining redundant links and joints.
- Kinematics of SLE based deployable structures.
- Statics of SLE based deployable structures.
- Summary

[5] This Lecture is based on material from Nagaraj (2009) and Nagaraj et al. (2009, 2010). Please see these and reference listed at the end for more details.

Contents of Lecture[5]

- Introduction
- Over-constrained mechanisms and deployable structures.
- Constraint Jacobian and obtaining redundant links and joints.
- Kinematics of SLE based deployable structures.
- Statics of SLE based deployable structures.
- Summary

[5] This Lecture is based on material from Nagaraj (2009) and Nagaraj et al. (2009, 2010). Please see these and reference listed at the end for more details.

Contents of Lecture[5]

- Introduction
- Over-constrained mechanisms and deployable structures.
- Constraint Jacobian and obtaining redundant links and joints.
- Kinematics of SLE based deployable structures.
- Statics of SLE based deployable structures.
- Summary

[5] This Lecture is based on material from Nagaraj (2009) and Nagaraj et al. (2009, 2010). Please see these and reference listed at the end for more details.

INTRODUCTION

- Large deployable structures
  - Space applications — small payload bay.
  - Modern communication and other satellites in orbit have large appendages.
  - Compact folded state in payload bay$\rightarrow$ Large deployed state in orbit.
- Large number of links and joints present.
  - In stowed state — locked/strapped one DOF mechanism.
  - During deployment, behaves as a one degree of freedom mechanism.
  - At the end of deployment, actuated joint is locked.
  - In deployed state — Structure capable of taking load.
- Main ones: coilable and pantograph masts, antennae and solar panels.
- This lecture deals with pantograph based deployable structures.

INTRODUCTION

- Large deployable structures
  - Space applications — small payload bay.
  - Modern communication and other satellites in orbit have large appendages.
  - Compact folded state in payload bay$\rightarrow$ Large deployed state in orbit.
- Large number of links and joints present.
  - In stowed state — locked/strapped one DOF mechanism.
  - During deployment, behaves as a one degree of freedom mechanism.
  - At the end of deployment, actuated joint is locked.
  - In deployed state — Structure capable of taking load.
- Main ones: coilable and pantograph masts, antennae and solar panels.
- This lecture deals with pantograph based deployable structures.

INTRODUCTION

- Large deployable structures
  - Space applications — small payload bay.
  - Modern communication and other satellites in orbit have large appendages.
  - Compact folded state in payload bay$\rightarrow$ Large deployed state in orbit.
- Large number of links and joints present.
  - In stowed state — locked/strapped one DOF mechanism.
  - During deployment, behaves as a one degree of freedom mechanism.
  - At the end of deployment, actuated joint is locked.
  - In deployed state — Structure capable of taking load.
- Main ones: coilable and pantograph masts, antennae and solar panels.
- This lecture deals with pantograph based deployable structures.

INTRODUCTION

- Large deployable structures
  - Space applications — small payload bay.
  - Modern communication and other satellites in orbit have large appendages.
  - Compact folded state in payload bay$\rightarrow$ Large deployed state in orbit.
- Large number of links and joints present.
  - In stowed state — locked/strapped one DOF mechanism.
  - During deployment, behaves as a one degree of freedom mechanism.
  - At the end of deployment, actuated joint is locked.
  - In deployed state — Structure capable of taking load.
- Main ones: coilable and pantograph masts, antennae and solar panels.
- This lecture deals with pantograph based deployable structures.

INTRODUCTION

EXAMPLES OF DEPLOYABLE STRUCTURES

Figure 45: Folded articulated square mast (FAST)

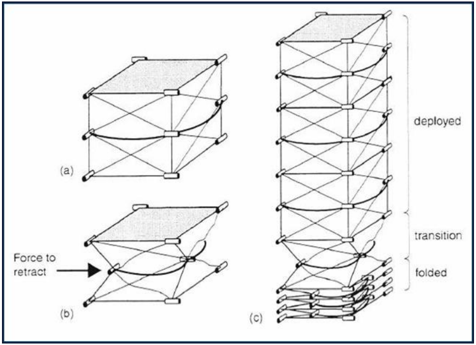

Figure 46: Deployment of FAST (see Warden 1987)

- Eight FAST masts are used in the International Space Station to support solar arrays.
- Source: AEC-Able Engineering Company, Inc.

INTRODUCTION

EXAMPLES OF DEPLOYABLE STRUCTURES

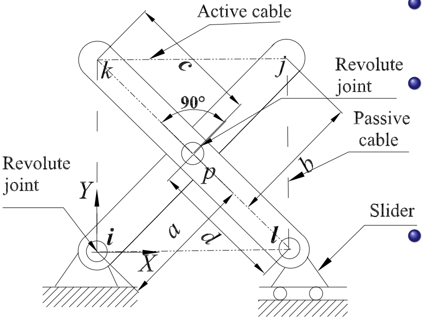

Figure 47: Planar scissor-like-element (SLE) or a pantograph

- Revolute joint in middle connects two links of equal length.
- Passive cable: connects two points such that it is slack when fully or partially folded and becomes taught when fully deployed.
- Passive cable(s) terminate deployment and increase stiffness of structure – sometimes more than one passive cables.
- Active cable: length decreases continuously and control deployment.

- Typically only one active cable — to avoid multiple mechanisms and actuators.
- Initially points (k, j) are close to (i, l) – As the active cable is shortened, (j, l) comes near to (k, i).

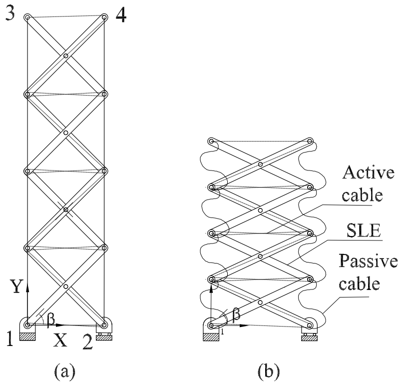

Figure 48: Stacked planar SLE masts (a) Fully deployed, (b) Partially deployed

- Four SLE's stacked on top of each other.
- Deployment angle varies from fully folded ($\beta = 0^\circ$) to fully deployed ($\beta = 45^\circ$).
- 8 passive cables and one active cable.

INTRODUCTION

EXAMPLES OF DEPLOYABLE STRUCTURES

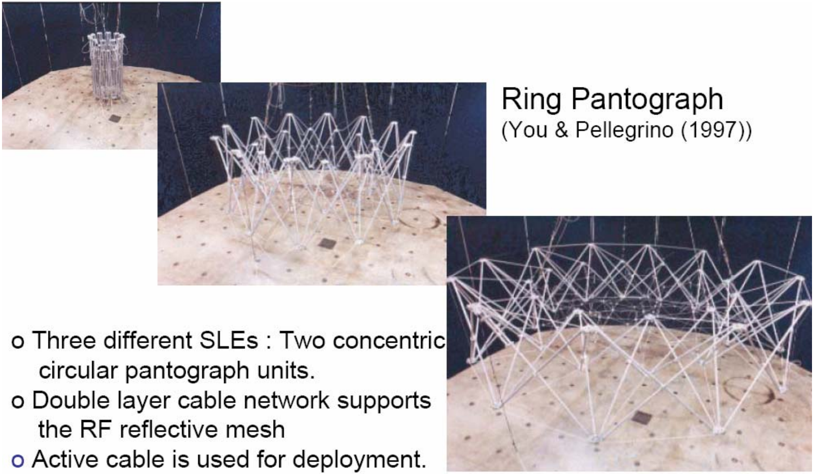

Figure 49: Deployment sequence of a cable stiffened pantograph deployable antennae (You & Pellegrin (1997)

Introduction

Examples of deployable structures

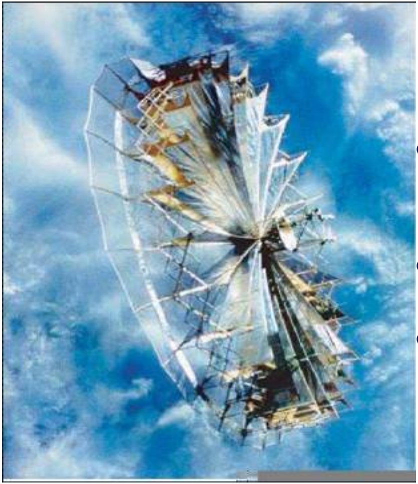

Figure 50: Schematic of a 5.6 m EGS antennae

- Circular pantograph ring and radial tensioned membrane rib connected to a central hub.
- 5.6 m by 6.4 m elliptical version tested in MIR space station.
- Made by Energia-GPI Space (EGS), Russia. Visit website for more information.

Over-constrained Mechanisms

Examples

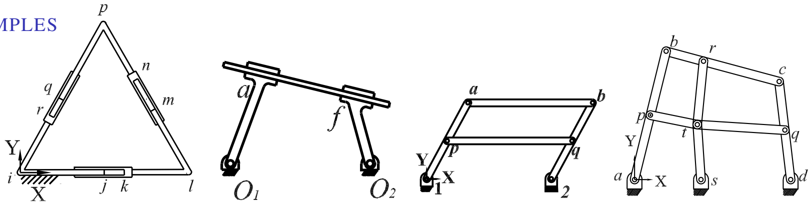

(a) 3 sliders (Mallik et al. 1994)

(b) RPPR mechanism

(c) Parallelogram linkage

(d) Kempes-Burmester focal mechanism (Wunderlich (1968)

Figure 51: Over-constrained Mechanisms

- Most well known DOF or mobility equation: Grübler-Kutzbach

$$M = \lambda(n - j - 1) + \sum_{i=1}^{j} f_i, \quad \lambda = 3 \text{ or} 6$$

- $M \neq 1$ in all example, although all can move!!
- Case (a): Special geometry, Case (b): Passive DOF along *PP* line *af*, Case (c): Redundant link *pq*, and Case (d): Redundant R joint at *d*.

DEGREE OF FREEDOM & MOBILITY

- Many other well-known mechanisms – Bennett mechanism (Bennett, 1903), deployable pantograph masts – gives $M \neq 1$ by Grübler-Kutzbach formula.
- Grübler-Kutzbach fails since special geometry is not taken in to account $\rightarrow$ Formula based on counting alone!!
- Many attempts to derive a "more universal" DOF/mobility formula (see Gogu, 2005)
- Passive DOF f_p subtracted by Tsai (2001): $S - S$ pair or $P - P$ pair cases.
- Equivalent screw system to choose λ (Waldron, 1966).
- Null space of Jacobian matrix (Freudenstein, 1962): $M = \mathrm{Nullity}([J])$ – Used in this Lecture!!
- Including state of self-stress s and number of internal mechanisms m (Guest and Fowler, 2005).

- Many other well-known mechanisms – Bennett mechanism (Bennett, 1903), deployable pantograph masts – gives $M \neq 1$ by Grübler-Kutzbach formula.
- Grübler-Kutzbach fails since special geometry is not taken in to account $\rightarrow$ Formula based on counting alone!!
- Many attempts to derive a "more universal" DOF/mobility formula (see Gogu, 2005)
- Passive DOF f_p subtracted by Tsai (2001): $S-S$ pair or $P-P$ pair cases.
- Equivalent screw system to choose λ (Waldron, 1966).
- Null space of Jacobian matrix (Freudenstein, 1962): $M = \text{Nullity}([J])$ – Used in this Lecture!!
- Including state of self-stress s and number of internal mechanisms m (Guest and Fowler, 2005).

Over-constrained Mechanisms and Deployable Structures

Degree of Freedom & Mobility

- Many other well-known mechanisms – Bennett mechanism (Bennett, 1903), deployable pantograph masts – gives $M \neq 1$ by Grübler-Kutzbach formula.
- Grübler-Kutzbach fails since special geometry is not taken in to account $\rightarrow$ Formula based on counting alone!!
- Many attempts to derive a "more universal" DOF/mobility formula (see Gogu, 2005)
- Passive DOF f_p subtracted by Tsai (2001): $S-S$ pair or $P-P$ pair cases.
- Equivalent screw system to choose λ (Waldron, 1966).
- Null space of Jacobian matrix (Freudenstein, 1962): $M = \mathrm{Nullity}([J])$ – Used in this Lecture!!
- Including state of self-stress s and number of internal mechanisms m (Guest and Fowler, 2005).

- Many other well-known mechanisms – Bennett mechanism (Bennett, 1903), deployable pantograph masts – gives $M \neq 1$ by Grübler-Kutzbach formula.
- Grübler-Kutzbach fails since special geometry is not taken in to account $\rightarrow$ Formula based on counting alone!!
- Many attempts to derive a "more universal" DOF/mobility formula (see Gogu, 2005)
- Passive DOF f_p subtracted by Tsai (2001): $S - S$ pair or $P - P$ pair cases.
- Equivalent screw system to choose λ (Waldron, 1966).
- Null space of Jacobian matrix (Freudenstein, 1962): $M = \mathrm{Nullity}([J])$ – Used in this Lecture!!
- Including state of self-stress s and number of internal mechanisms m (Guest and Fowler, 2005).

- Many other well-known mechanisms – Bennett mechanism (Bennett, 1903), deployable pantograph masts – gives $M \neq 1$ by Grübler-Kutzbach formula.
- Grübler-Kutzbach fails since special geometry is not taken in to account $\rightarrow$ Formula based on counting alone!!
- Many attempts to derive a "more universal" DOF/mobility formula (see Gogu, 2005)
- Passive DOF f_p subtracted by Tsai (2001): $S-S$ pair or $P-P$ pair cases.
- Equivalent screw system to choose λ (Waldron, 1966).
- Null space of Jacobian matrix (Freudenstein, 1962): $M = \text{Nullity}([J])$ – Used in this Lecture!!
- Including state of self-stress s and number of internal mechanisms m (Guest and Fowler, 2005).

Over-constrained Mechanisms and Deployable Structures

Degree of Freedom & Mobility

- Many other well-known mechanisms – Bennett mechanism (Bennett, 1903), deployable pantograph masts – gives $M \neq 1$ by Grübler-Kutzbach formula.
- Grübler-Kutzbach fails since special geometry is not taken in to account $\rightarrow$ Formula based on counting alone!!
- Many attempts to derive a "more universal" DOF/mobility formula (see Gogu, 2005)
- Passive DOF f_p subtracted by Tsai (2001): $S-S$ pair or $P-P$ pair cases.
- Equivalent screw system to choose λ (Waldron, 1966).
- Null space of Jacobian matrix (Freudenstein, 1962): $M = \mathrm{Nullity}([J])$ – Used in this Lecture!!
- Including state of self-stress s and number of internal mechanisms m (Guest and Fowler, 2005).

Over-constrained Mechanisms and Deployable Structures

Degree of Freedom & Mobility

- Many other well-known mechanisms – Bennett mechanism (Bennett, 1903), deployable pantograph masts – gives $M \neq 1$ by Grübler-Kutzbach formula.
- Grübler-Kutzbach fails since special geometry is not taken in to account $\rightarrow$ Formula based on counting alone!!
- Many attempts to derive a "more universal" DOF/mobility formula (see Gogu, 2005)
- Passive DOF f_p subtracted by Tsai (2001): $S-S$ pair or $P-P$ pair cases.
- Equivalent screw system to choose λ (Waldron, 1966).
- Null space of Jacobian matrix (Freudenstein, 1962): $M = \mathrm{Nullity}([J])$ – Used in this Lecture!!
- Including state of self-stress s and number of internal mechanisms m (Guest and Fowler, 2005).

DIFFERENT TYPES OF COORDINATES

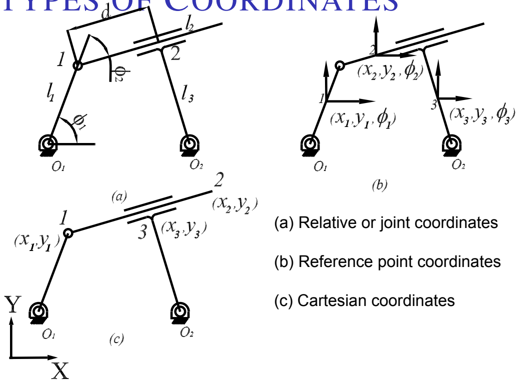

Figure 52: Three kinds of coordinates in RRPR mechanism

- Relative coordinates are described with respect to previous link (Denavit and Hartenberg, 1965).
- Reference point (or *absolute*) coordinates – planar body with 3 coordinate (x, y, ϕ) and by 6 coordinates in space (Nikravesh, 1988).
- Cartesian (or *natural* coordinates) – reference point moved to joint (Garcia de Jalon and Bayo, 1994).

Different types of Coordinates

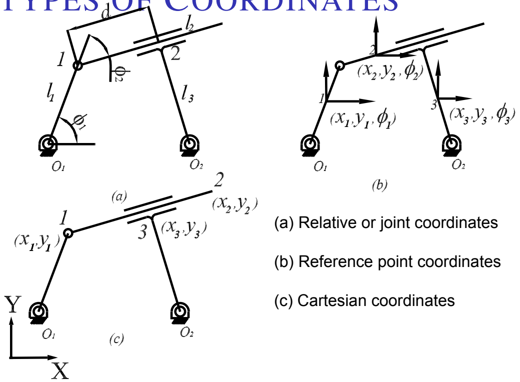

Figure 52: Three kinds of coordinates in RRPR mechanism

- Relative coordinates are described with respect to previous link (Denavit and Hartenberg, 1965).
- Reference point (or *absolute*) coordinates – planar body with 3 coordinate (x, y, ϕ) and by 6 coordinates in space (Nikravesh, 1988).
- Cartesian (or *natural* coordinates) – reference point moved to joint (Garcia de Jalon and Bayo, 1994).

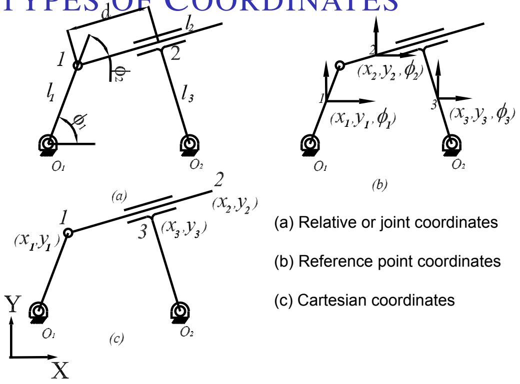

Figure 52: Three kinds of coordinates in RRPR mechanism

- Relative coordinates are described with respect to previous link (Denavit and Hartenberg, 1965).
- Reference point (or *absolute*) coordinates – planar body with 3 coordinate (x, y, ϕ) and by 6 coordinates in space (Nikravesh, 1988).
- Cartesian (or *natural* coordinates) – reference point moved to joint (Garcia de Jalon and Bayo, 1994).

Coordinates and Constraints

- Constraint equations are different for different choice of coordinates.
- For relative coordinates loop-closure constraints (see Module 4, Lecture 1) for RRPR mechanism

$$l_1 \cos\phi_1 + d\cos(\phi_1+\phi_2) + l_3\cos(\phi_1+\phi_2-\pi/2) = l_4$$
$$l_1 \sin\phi_1 + d\sin(\phi_1+\phi_2) + l_3\sin(\phi_1+\phi_2-\pi/2) = 0$$

  where $\mathbf{q} = (\phi_1, \phi_2, d)$ are the coordinates (see figure).
- For reference point coordinates, the constrains are

$$x_a + l_1/2\cos\phi_1 = x_1,\ y_a + l_1/2\sin\phi_1 = y_1$$
$$x_1 + l_1/2\cos\phi_1 + l_2/2\cos\phi_2 = x_2,\ y_1 + l_1/2\sin\phi_1 + l_2/2\sin\phi_2 = y_2$$
$$\phi_2 - \phi_3 = \pi/2,\ (y_2 - y_3)\cos\phi_2 + (x_3 - x_2)\sin\phi_2 = l_3/2$$
$$x_3 + l_3/2\cos\phi_3 = x_d,\ y_3 + l_3/2\sin\phi_3 = y_d$$

  where $\mathbf{q} = (x_1, y_1, \phi_1, x_2, y_2, \phi_2, x_3, y_3, \phi_3)$ are the coordinates (see figure).
- For Cartesian coordinates

$$(x_1 - x_a)^2 + (y_1 - y_a)^2 = {l_1}^2,\ (x_2 - x_1)^2 + (y_2 - y_1)^2 = {l_2}^2$$
$$(x_3 - x_b)^2 + (y_3 - y_b)^2 = {l_3}^2,\ (x_2 - x_1)(x_3 - x_b) + (y_2 - y_1)(y_3 - y_b) = l_2 l_3 \cos\phi$$
$$(x_3 - x_1)/(x_2 - x_1) - (y_3 - y_1)/(y_2 - y_1) = 0$$

  where $\mathbf{q} = (x_1, y_1, x_2, y_2, x_3, y_3)$ are the coordinates (see figure).

Coordinates and Constraints

- Constraint equations are different for different choice of coordinates.
- For relative coordinates loop-closure constraints (see Module 4, Lecture 1) for RRPR mechanism

$$l_1 \cos\phi_1 + d\cos(\phi_1+\phi_2) + l_3\cos(\phi_1+\phi_2-\pi/2) = l_4$$
$$l_1 \sin\phi_1 + d\sin(\phi_1+\phi_2) + l_3\sin(\phi_1+\phi_2-\pi/2) = 0$$

where $\mathbf{q} = (\phi_1, \phi_2, d)$ are the coordinates (see figure).

- For reference point coordinates, the constrains are

$$x_a + l_1/2\cos\phi_1 = x_1,\ \ y_a + l_1/2\sin\phi_1 = y_1$$
$$x_1 + l_1/2\cos\phi_1 + l_2/2\cos\phi_2 = x_2,\ \ y_1 + l_1/2\sin\phi_1 + l_2/2\sin\phi_2 = y_2$$
$$\phi_2 - \phi_3 = \pi/2,\ \ (y_2 - y_3)\cos\phi_2 + (x_3 - x_2)\sin\phi_2 = l_3/2$$
$$x_3 + l_3/2\cos\phi_3 = x_d,\ \ y_3 + l_3/2\sin\phi_3 = y_d$$

where $\mathbf{q} = (x_1, y_1, \phi_1, x_2, y_2, \phi_2, x_3, y_3, \phi_3)$ are the coordinates (see figure).

- For Cartesian coordinates

$$(x_1 - x_a)^2 + (y_1 - y_a)^2 = l_1{}^2,\ \ (x_2 - x_1)^2 + (y_2 - y_1)^2 = l_2{}^2$$
$$(x_3 - x_b)^2 + (y_3 - y_b)^2 = l_3{}^2,\ \ (x_2 - x_1)(x_3 - x_b) + (y_2 - y_1)(y_3 - y_b) = l_2 l_3 \cos\phi$$
$$(x_3 - x_1)/(x_2 - x_1) - (y_3 - y_1)/(y_2 - y_1) = 0$$

where $\mathbf{q} = (x_1, y_1, x_2, y_2, x_3, y_3)$ are the coordinates (see figure).

- Constraint equations are different for different choice of coordinates.
- For relative coordinates loop-closure constraints (see Module 4, Lecture 1) for RRPR mechanism

$$
\begin{aligned}
l_1 \cos\phi_1 + d\cos(\phi_1+\phi_2) + l_3\cos(\phi_1+\phi_2-\pi/2) &= l_4 \\
l_1 \sin\phi_1 + d\sin(\phi_1+\phi_2) + l_3\sin(\phi_1+\phi_2-\pi/2) &= 0
\end{aligned}
$$

where $\mathbf{q} = (\phi_1, \phi_2, d)$ are the coordinates (see figure).

- For reference point coordinates, the constrains are

$$
\begin{aligned}
& x_a + l_1/2\cos\phi_1 = x_1,\ y_a + l_1/2\sin\phi_1 = y_1 \\
& x_1 + l_1/2\cos\phi_1 + l_2/2\cos\phi_2 = x_2,\ y_1 + l_1/2\sin\phi_1 + l_2/2\sin\phi_2 = y_2 \\
& \phi_2 - \phi_3 = \pi/2,\ (y_2-y_3)\cos\phi_2 + (x_3-x_2)\sin\phi_2 = l_3/2 \\
& x_3 + l_3/2\cos\phi_3 = x_d,\ y_3 + l_3/2\sin\phi_3 = y_d
\end{aligned}
$$

where $\mathbf{q} = (x_1, y_1, \phi_1, x_2, y_2, \phi_2, x_3, y_3, \phi_3)$ are the coordinates (see figure).

- For Cartesian coordinates

$$
\begin{aligned}
& (x_1-x_a)^2 + (y_1-y_a)^2 = l_1{}^2,\ (x_2-x_1)^2 + (y_2-y_1)^2 = l_2{}^2 \\
& (x_3-x_b)^2 + (y_3-y_b)^2 = l_3{}^2,\ (x_2-x_1)(x_3-x_b) + (y_2-y_1)(y_3-y_b) = l_2 l_3 \cos\phi \\
& (x_3-x_1)/(x_2-x_1) - (y_3-y_1)/(y_2-y_1) = 0
\end{aligned}
$$

where $\mathbf{q} = (x_1, y_1, x_2, y_2, x_3, y_3)$ are the coordinates (see figure).

Coordinates and Constraints

- Constraint equations are different for different choice of coordinates.
- For relative coordinates loop-closure constraints (see Module 4, Lecture 1) for RRPR mechanism

$$
\begin{aligned}
l_1 \cos\phi_1 + d\cos(\phi_1+\phi_2) + l_3\cos(\phi_1+\phi_2-\pi/2) &= l_4 \\
l_1 \sin\phi_1 + d\sin(\phi_1+\phi_2) + l_3\sin(\phi_1+\phi_2-\pi/2) &= 0
\end{aligned}
$$

  where $\mathbf{q} = (\phi_1, \phi_2, d)$ are the coordinates (see figure).
- For reference point coordinates, the constrains are

$$
\begin{aligned}
& x_a + l_1/2\cos\phi_1 = x_1,\ \ y_a + l_1/2\sin\phi_1 = y_1 \\
& x_1 + l_1/2\cos\phi_1 + l_2/2\cos\phi_2 = x_2,\ \ y_1 + l_1/2\sin\phi_1 + l_2/2\sin\phi_2 = y_2 \\
& \phi_2 - \phi_3 = \pi/2,\ \ (y_2 - y_3)\cos\phi_2 + (x_3 - x_2)\sin\phi_2 = l_3/2 \\
& x_3 + l_3/2\cos\phi_3 = x_d,\ \ y_3 + l_3/2\sin\phi_3 = y_d
\end{aligned}
$$

  where $\mathbf{q} = (x_1, y_1, \phi_1, x_2, y_2, \phi_2, x_3, y_3, \phi_3)$ are the coordinates (see figure).
- For Cartesian coordinates

$$
\begin{aligned}
& (x_1 - x_a)^2 + (y_1 - y_a)^2 = l_1{}^2,\ \ (x_2 - x_1)^2 + (y_2 - y_1)^2 = l_2{}^2 \\
& (x_3 - x_b)^2 + (y_3 - y_b)^2 = l_3{}^2,\ \ (x_2 - x_1)(x_3 - x_b) + (y_2 - y_1)(y_3 - y_b) = l_2 l_3 \cos\phi \\
& (x_3 - x_1)/(x_2 - x_1) - (y_3 - y_1)/(y_2 - y_1) = 0
\end{aligned}
$$

  where $\mathbf{q} = (x_1, y_1, x_2, y_2, x_3, y_3)$ are the coordinates (see figure).

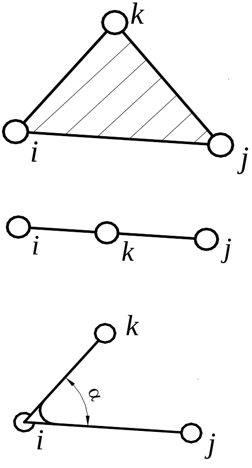

Figure 53: Constraints associated with rigid link

- Distance between two points remain constant: $\mathbf{r}_{ij} \cdot \mathbf{r}_{ij} = {L_{ij}}^2$
- Link with three points: distance btween i, j and k remain constant.
- Link with 3 co-linear points: $\mathbf{r}_{ij} \cdot \mathbf{r}_{ij} = {L_{ij}}^2$ and $\mathbf{r}_{ij} - k\mathbf{r}_{ik} = \mathbf{0}$.
- Link with three points and included angle.

$$\begin{aligned}
\mathbf{r}_{ij} \cdot \mathbf{r}_{ij} &= {L_{ij}}^2 \\
\mathbf{r}_{ik} \cdot \mathbf{r}_{ik} &= {L_{ik}}^2 \\
\mathbf{r}_{ij} \cdot \mathbf{r}_{ik} &= L_{ij} L_{ik} \cos(\alpha)
\end{aligned}$$

Constraints with Natural Coordinates

Joints

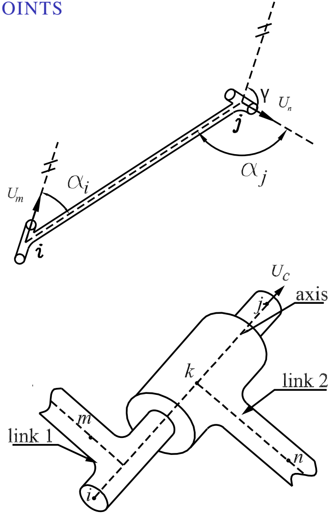

Figure 54: Constraints associated with joints

- Spherical joint – two adjacent links share a point.
- Rotary joint constraints

$$\mathbf{r}_{ij} \cdot \mathbf{u}_m - L_{ij}\cos(\alpha_i) = 0$$
$$\mathbf{r}_{ij} \cdot \mathbf{u}_n - L_{ij}\cos(\alpha_j) = 0$$
$$\mathbf{r}_{ij} \cdot \mathbf{r}_{ij} = L_{ij}^2, \ \mathbf{u}_n \cdot \mathbf{u}_m = \cos(\gamma)$$
$$\mathbf{u}_n \cdot \mathbf{u}_n = \mathbf{u}_m \cdot \mathbf{u}_m = 1$$

γ is the angle shown in figure.

- Cylindrical joint constraint

$$\mathbf{r}_{ik} \times \mathbf{r}_{ij} = 0$$
$$\mathbf{r}_{ij} \times \mathbf{u}_c = 0$$

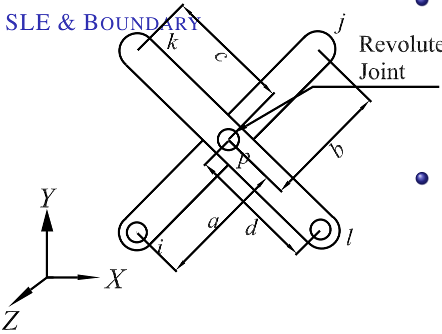

Figure 55: Constraints associated with SLE

- Two length constraint equations

$$
\begin{aligned}
\mathbf{r}_{ij} \cdot \mathbf{r}_{ij} &= L_{ij}^2 \\
\mathbf{r}_{kl} \cdot \mathbf{r}_{kl} &= L_{kl}^2
\end{aligned}
$$

- Two co-linearity constraints

$$
\begin{aligned}
\mathbf{r}_{ij} - \lambda_1 \mathbf{r}_{ip} &= 0 \\
\mathbf{r}_{kl} - \lambda_2 \mathbf{r}_{kp} &= 0
\end{aligned}
$$

$\lambda_1 = \frac{a+b}{a}$ and $\lambda_2 = \frac{c+d}{c}$.

- Simplifying, SLE constraints are

$$\frac{b}{a+b}\mathbf{P}_i + \frac{a}{a+b}\mathbf{P}_j - \frac{c}{c+d}\mathbf{P}_l - \frac{d}{c+d}\mathbf{P}_k = 0$$

$\mathbf{P}_m$ $(m = i,j,k,l)$ are the position vectors of 4 points.

- Boundary constraints: If point P is fixed, its coordinates are 0.

- Rigid, joint and boundary constraints *together* can be written as

$$f_j(X_1, Y_1, Z_1, X_2, \cdots, Y_n, Z_n) = 0 \quad \text{for } j = 1 \quad \text{to} \quad n_c$$

  n_c is the total number of constraint equations and $3n$ is the number of Cartesian coordinates of the system.

- Derivative of all constraint equations in symbolic form

$$[\mathbf{J}]\delta\mathbf{X} = \mathbf{0}$$

- Homogeneous equation $\Rightarrow$ Non-trivial $\delta\mathbf{X}$ if dimension of null space of $[J]$ is *at least* one.
- Dimension of null-space of $[J]$ *same as DOF* of mechanism!!

- Rigid, joint and boundary constraints *together* can be written as

$$f_j(X_1, Y_1, Z_1, X_2, \cdots, Y_n, Z_n) = 0 \quad \text{for } j = 1 \quad \text{to} \quad n_c$$

  n_c is the total number of constraint equations and $3n$ is the number of Cartesian coordinates of the system.

- Derivative of all constraint equations in symbolic form

$$[\mathbf{J}]\delta\mathbf{X} = \mathbf{0}$$

- Homogeneous equation $\Rightarrow$ Non-trivial $\delta\mathbf{X}$ if dimension of null space of $[J]$ is *at least* one.
- Dimension of null-space of $[J]$ *same as DOF* of mechanism!!

- Rigid, joint and boundary constraints *together* can be written as

$$f_j(X_1, Y_1, Z_1, X_2, \cdots, Y_n, Z_n) = 0 \quad \text{for } j = 1 \quad \text{to} \quad n_c$$

n_c is the total number of constraint equations and $3n$ is the number of Cartesian coordinates of the system.

- Derivative of all constraint equations in symbolic form

$$[\mathbf{J}]\delta\mathbf{X} = \mathbf{0}$$

- Homogeneous equation $\Rightarrow$ Non-trivial $\delta\mathbf{X}$ if dimension of null space of $[J]$ is *at least* one.
- Dimension of null-space of $[J]$ *same as DOF* of mechanism!!

- Rigid, joint and boundary constraints *together* can be written as

$$f_j(X_1, Y_1, Z_1, X_2, \cdots, Y_n, Z_n) = 0 \quad \text{for } j = 1 \quad \text{to} \quad n_c$$

  n_c is the total number of constraint equations and $3n$ is the number of Cartesian coordinates of the system.
- Derivative of all constraint equations in symbolic form

$$[\mathbf{J}]\delta\mathbf{X} = \mathbf{0}$$

- Homogeneous equation $\Rightarrow$ Non-trivial $\delta\mathbf{X}$ if dimension of null space of $[J]$ is *at least* one.
- Dimension of null-space of $[J]$ *same as DOF* of mechanism!!

Algorithm to obtain DOF

- Add the derivative of the constraint equations one at a time in the following order
  - arising out of length constraints
  - arising out of joint constraints
- At each step evaluate dimension of null-space of [J].
- Nullity([J]) doesn't decrease when a constraint is added $\rightarrow$ Constraint is redundant.
- Boundary constraints are added last: Nullity([J]) doesn't decrease $\rightarrow$ Boundary constraint is redundant.
- Final dimension of the null-space of [J] is the mobility/degree of freedom of the system.

Algorithm to obtain DOF

- Add the derivative of the constraint equations one at a time in the following order
  - arising out of length constraints
  - arising out of joint constraints
- At each step evaluate dimension of null-space of [**J**].
- Nullity([**J**]) doesn't decrease when a constraint is added $\rightarrow$ Constraint is redundant.
- Boundary constraints are added last: Nullity([**J**]) doesn't decrease $\rightarrow$ Boundary constraint is redundant.
- Final dimension of the null-space of [**J**] is the mobility/degree of freedom of the system.

Algorithm to obtain DOF

- Add the derivative of the constraint equations one at a time in the following order
  - arising out of length constraints
  - arising out of joint constraints
- At each step evaluate dimension of null-space of [**J**].
- Nullity([**J**]) doesn't decrease when a constraint is added → Constraint is redundant.
- Boundary constraints are added last: Nullity([**J**]) doesn't decrease → Boundary constraint is redundant.
- Final dimension of the null-space of [**J**] is the mobility/degree of freedom of the system.

Algorithm to obtain DOF

- Add the derivative of the constraint equations one at a time in the following order
  - arising out of length constraints
  - arising out of joint constraints
- At each step evaluate dimension of null-space of [**J**].
- $\text{Nullity}([\mathbf{J}])$ doesn't decrease when a constraint is added $\rightarrow$ Constraint is redundant.
- Boundary constraints are added last: $\text{Nullity}([\mathbf{J}])$ doesn't decrease $\rightarrow$ Boundary constraint is redundant.
- Final dimension of the null-space of [J] is the mobility/degree of freedom of the system.

ALGORITHM TO OBTAIN DOF

- Add the derivative of the constraint equations one at a time in the following order
  - arising out of length constraints
  - arising out of joint constraints
- At each step evaluate dimension of null-space of $[\mathbf{J}]$.
- $\text{Nullity}([\mathbf{J}])$ doesn't decrease when a constraint is added $\rightarrow$ Constraint is redundant.
- Boundary constraints are added last: $\text{Nullity}([\mathbf{J}])$ doesn't decrease $\rightarrow$ Boundary constraint is redundant.
- Final dimension of the null-space of $[\mathbf{J}]$ is the mobility/degree of freedom of the system.

Examples

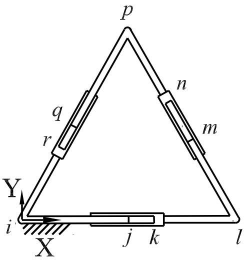

Constraints	Size of [J]	Nullspace	Remarks
Length constraints + Cross products	(12,18)	6	
+ Dot product for the link $r-i-j$	(13,18)	5	
+ Dot product for the link $k-l-m$	(14,18)	4	
+ Dot product for the link $n-p-q$	(15,18)	4	Redundant
+ Boundary conditions ($X_i = Y_i = 0$)	(17,12)	2	
+ Boundary condition ($Y_l = 0$)	(18,18)	1	

Figure 56: Constraints Jacobian analysis of three slider mechanism

- Constraint Jacobian analysis correctly predicts DOF as 1.
- Also determines *redundant* constraints which resulted in $M \neq 1$.

KINEMATIC ANALYSIS OF OVER-CONSTRAINED MECHANISMS

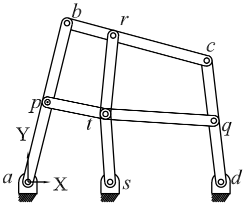

Constraints	Size of [J]	Nullspace	Remarks
Length constraints	(10,12)	2	
+ Cross products	(13,12)	1	
$a-p-b, b-r-c$ and $c-q-d$			Two cross products redundant
Joint d removed			
Length constraints	(10,14)	4	
+ Cross product	(13,14)	1	
$a-p-b, b-r-c$ and $c-q-d$			

Nullspace magnitude	Variables	Nullspace magnitude	Variables	Remarks
-0.1740	X_p	-0.1740	X_p	
0.3013	Y_p	0.3013	Y_p	
-0.3480	X_b	-0.3480	X_b	
0.6027	Y_b	0.6027	Y_b	
0.0085	X_r	0.0085	X_r	
0.2921	Y_r	0.2921	Y_r	
0.3650	X_c	0.3650	X_c	
-0.0185	Y_c	-0.0185	Y_c	
0.1825	X_q	0.1825	X_q	
-0.0092	Y_q	-0.0092	Y_q	
-0.1660	X_t	-0.1660	X_t	
0.3387	Y_t	0.3387	Y_t	
-	-	0.0000	X_d	Redundant
-	-	0.0000	Y_d	Redundant

Joint *d* is seen to be redundant

Link *cd* rotates about *d* without a joint at *d* !!

Figure 57: Constraints Jacobian analysis of Kempes -Burmester mechanism

Kinematic Analysis of SLE based Masts

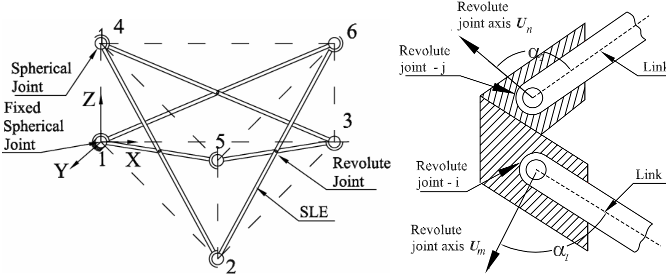

Constraints	Size of [J]	Nullspace	Remarks
Length constraints	(6,18)	12	
Revolute joints			
+ FACE 1	(8,18)	10	
+ FACE 2	(10,18)	8	
+ FACE 3	(12,18)	6	
SLEs			
+ SLE 1	(15,18)	4	
+ SLE 2	(18,18)	4	SLE - 2 is redundant
+ SLE 3	(21,18)	4	SLE - 3 is redundant
+ Boundary conditions $X_1 = Y_1 = Z_1 = 0$	(24,18)	1	

Spherical joint replaced with Revolute joint shown above

SLE - 2 and 3 are redundant
DOF is 1 without SLE - 2 and SLE - 3

Figure 58: Constraints Jacobian analysis of triangular SLE mast with revolute joints

Kinematic Analysis of SLE based Masts

Examples

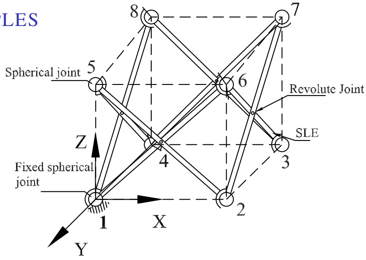

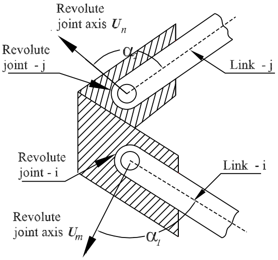

Constraints	Size of [J]	Nullspace	Remarks
Length constraints	(8,24)	16	
Revolute joints			
+ FACE 1	(10,24)	14	
+ FACE 2	(12,24)	12	
+ FACE 3	(14,24)	10	
+ FACE 4	(16,24)	8	
SLEs			
+ SLE 1	(19,24)	5	
+ SLE 2	(22,24)	4	two components are redundant
+ SLE 3	(25,24)	4	SLE - 3 is redundant
+ SLE 4	(28,24)	4	SLE - 4 is redundant
+ Boundary conditions $X_1 = Y_1 = Z_1 = 0$	(31,24)	1	

Spherical joint replaced with Revolute joint shown above

SLE - 3 and 4 are redundant DOF is 1 without SLE - 3 and SLE - 4

Figure 59: Constraints Jacobian analysis of box SLE mast with revolute joints

Examples

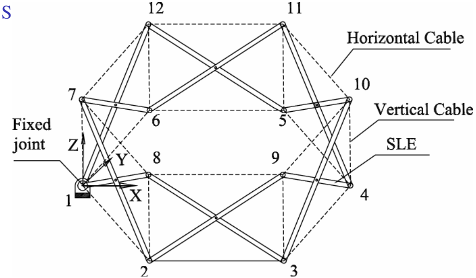

Contents	Size of [J]	Null Space	Remarks
+ SLE 1	(20,39)	21	
+ SLE 2	(28,42)	18	
+ SLE 3	(36,45)	15	
+ SLE 4	(44,48)	12	
+ SLE 5	(52,51)	10	
+ SLE 6	(60,54)	10	SLE - 6 is redundant
+ FACE 1	(62,54)	8	
+ FACE 2	(64,54)	6	
+ FACE 3	(66,54)	5	
+ FACE 4	(68,54)	4	
+ FACE 5	(70,54)	4	Revolute joints are redundant
+ FACE 6	(72,54)	4	Revolute joints are redundant
+ Boundary conditions ($X_1 = Y_1 = Z_1 = 0$)	(75,54)	1	Mechanism
+ Cable 1-2	(76,54)	0	Structure

SLE – 6 and R joints on FACE 5 & 6 are redundant
DOF is 1 without Cable
DOF is 0 with Cable
(modeled as rigid rod)

Figure 60: Constraints Jacobian analysis of hexagonal SLE mast with cables

- Once redundancy identified $\rightarrow$ Can solve kinematics!
- $L = 30.0$, Joint 2 moves horizontally and height decreases!!

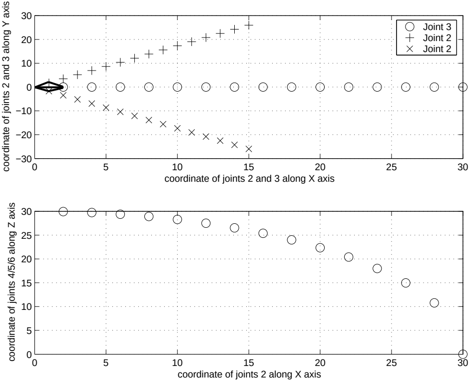

Figure 61: Trajectory of joint coordinates for a triangular mast

Summary of Kinematic Analysis of Over-constrained Mechanisms

- Over-constrained mechanisms do not give correct DOF from Grübler-Kutzbach criterion.
- Grübler-Kutzbach criterion does not take into account geometry!
- Null space dimension of the constraint Jacobian
  - Correctly determines degrees of freedom.
  - Can identify redundant links, joints and boundary conditions.
- Constraint Jacobian approach is *local* – results valid at a chosen configuration & does not account for *singularities*.
- Global analysis possible for pantograph masts and simple mechanisms.
- Constraint Jacobian approach applied to SLE based masts – *redundant* SLE's can be identified!

SUMMARY OF KINEMATIC ANALYSIS OF OVER-CONSTRAINED MECHANISMS

- Over-constrained mechanisms do not give correct DOF from Grübler-Kutzbach criterion.
- Grübler-Kutzbach criterion does not take into account geometry!
- Null space dimension of the constraint Jacobian
  - Correctly determines degrees of freedom.
  - Can identify redundant links, joints and boundary conditions.
- Constraint Jacobian approach is *local* – results valid at a chosen configuration & does not account for *singularities*.
- Global analysis possible for pantograph masts and simple mechanisms.
- Constraint Jacobian approach applied to SLE based masts – *redundant* SLE's can be identified!

Summary of Kinematic Analysis of Over-constrained Mechanisms

- Over-constrained mechanisms do not give correct DOF from Grübler-Kutzbach criterion.
- Grübler-Kutzbach criterion does not take into account geometry!
- Null space dimension of the constraint Jacobian
  - Correctly determines degrees of freedom.
  - Can identify redundant links, joints and boundary conditions.
- Constraint Jacobian approach is *local* – results valid at a chosen configuration & does not account for *singularities*.
- Global analysis possible for pantograph masts and simple mechanisms.
- Constraint Jacobian approach applied to SLE based masts – *redundant* SLE's can be identified!

Summary of Kinematic Analysis of Over-constrained Mechanisms

- Over-constrained mechanisms do not give correct DOF from Grübler-Kutzbach criterion.
- Grübler-Kutzbach criterion does not take into account geometry!
- Null space dimension of the constraint Jacobian
  - Correctly determines degrees of freedom.
  - Can identify redundant links, joints and boundary conditions.
- Constraint Jacobian approach is *local* – results valid at a chosen configuration & does not account for *singularities*.
- Global analysis possible for pantograph masts and simple mechanisms.
- Constraint Jacobian approach applied to SLE based masts – *redundant* SLE's can be identified!

Summary of Kinematic Analysis of Over-constrained Mechanisms

- Over-constrained mechanisms do not give correct DOF from Grübler-Kutzbach criterion.
- Grübler-Kutzbach criterion does not take into account geometry!
- Null space dimension of the constraint Jacobian
  - Correctly determines degrees of freedom.
  - Can identify redundant links, joints and boundary conditions.
- Constraint Jacobian approach is *local* – results valid at a chosen configuration & does not account for *singularities*.
- Global analysis possible for pantograph masts and simple mechanisms.
- Constraint Jacobian approach applied to SLE based masts – *redundant* SLE's can be identified!

Summary of Kinematic Analysis of Over-constrained Mechanisms

- Over-constrained mechanisms do not give correct DOF from Grübler-Kutzbach criterion.
- Grübler-Kutzbach criterion does not take into account geometry!
- Null space dimension of the constraint Jacobian
  - Correctly determines degrees of freedom.
  - Can identify redundant links, joints and boundary conditions.
- Constraint Jacobian approach is *local* – results valid at a chosen configuration & does not account for *singularities*.
- Global analysis possible for pantograph masts and simple mechanisms.
- Constraint Jacobian approach applied to SLE based masts – *redundant* SLE's can be identified!

- At the end of deployment, the actuator is locked & Mechanism becomes a structure.
- Various approaches to analyse structures (see Kwan & Pellegrino (1994), Shan (1992) and Gantes et al. (1994))
- Constraint Jacobian matrix extended for static analysis.
- Stiffness matrix obtained from each type of constraints and then assembled.
- Rank of system stiffness matrix gives redundant links and joints.
- Deflection analysis from stiffness matrix.

- At the end of deployment, the actuator is locked & Mechanism becomes a structure.
- Various approaches to analyse structures (see Kwan & Pellegrino (1994), Shan (1992) and Gantes et al. (1994))
- Constraint Jacobian matrix extended for static analysis.
- Stiffness matrix obtained from each type of constraints and then assembled.
- Rank of system stiffness matrix gives redundant links and joints.
- Deflection analysis from stiffness matrix.

- At the end of deployment, the actuator is locked & Mechanism becomes a structure.
- Various approaches to analyse structures (see Kwan & Pellegrino (1994), Shan (1992) and Gantes et al. (1994))
- Constraint Jacobian matrix extended for static analysis.
- Stiffness matrix obtained from each type of constraints and then assembled.
- Rank of system stiffness matrix gives redundant links and joints.
- Deflection analysis from stiffness matrix.

- At the end of deployment, the actuator is locked & Mechanism becomes a structure.
- Various approaches to analyse structures (see Kwan & Pellegrino (1994), Shan (1992) and Gantes et al. (1994))
- Constraint Jacobian matrix extended for static analysis.
- Stiffness matrix obtained from each type of constraints and then assembled.
- Rank of system stiffness matrix gives redundant links and joints.
- Deflection analysis from stiffness matrix.

- At the end of deployment, the actuator is locked & Mechanism becomes a structure.
- Various approaches to analyse structures (see Kwan & Pellegrino (1994), Shan (1992) and Gantes et al. (1994))
- Constraint Jacobian matrix extended for static analysis.
- Stiffness matrix obtained from each type of constraints and then assembled.
- Rank of system stiffness matrix gives redundant links and joints.
- Deflection analysis from stiffness matrix.

- At the end of deployment, the actuator is locked & Mechanism becomes a structure.
- Various approaches to analyse structures (see Kwan & Pellegrino (1994), Shan (1992) and Gantes et al. (1994))
- Constraint Jacobian matrix extended for static analysis.
- Stiffness matrix obtained from each type of constraints and then assembled.
- Rank of system stiffness matrix gives redundant links and joints.
- Deflection analysis from stiffness matrix.

- For elastic members, $[\mathbf{S}_m]\delta\mathbf{L} = \delta\mathbf{T}$; Elongation is $\delta\mathbf{L}$ for a load $\delta\mathbf{T}$
- The member stiffness matrix is

$$[\mathbf{S}_m] = \begin{bmatrix} \frac{A_1 E_1}{l_1} & 0 & 0 & 0 \\ 0 & \frac{A_2 E_2}{l_2} & 0 & 0 \\ 0 & 0 & \frac{A_3 E_3}{l_3} & 0 \\ 0 & 0 & 0 & \frac{A_4 E_4}{l_4} \end{bmatrix}$$

  where l, A and E are length, cross-sectional area and elastic modulus, respectively.
- External force is related to $\delta\mathbf{T}$ by the Jacobian matrix: $[\mathbf{J}_m]^T \delta\mathbf{T} = \delta\mathbf{F}$
- Hence, $[\mathbf{J}_m]^T [\mathbf{S}_m][\mathbf{J}_m]\delta\mathbf{X} = \delta\mathbf{F}$.
- Elastic stiffness matrix is $[\mathbf{K}_m] = [\mathbf{J}_m]^T [\mathbf{S}_m][\mathbf{J}_m]$.

- For elastic members, $[\mathbf{S}_m]\delta\mathbf{L} = \delta\mathbf{T}$; Elongation is $\delta\mathbf{L}$ for a load $\delta\mathbf{T}$
- The member stiffness matrix is

$$[\mathbf{S}_m] = \begin{bmatrix} \frac{A_1 E_1}{l_1} & 0 & 0 & 0 \\ 0 & \frac{A_2 E_2}{l_2} & 0 & 0 \\ 0 & 0 & \frac{A_3 E_3}{l_3} & 0 \\ 0 & 0 & 0 & \frac{A_4 E_4}{l_4} \end{bmatrix}$$

  where l, A and E are length, cross-sectional area and elastic modulus, respectively.
- External force is related to $\delta\mathbf{T}$ by the Jacobian matrix: $[\mathbf{J}_m]^T\delta\mathbf{T} = \delta\mathbf{F}$
- Hence, $[\mathbf{J}_m]^T[\mathbf{S}_m][\mathbf{J}_m]\delta\mathbf{X} = \delta\mathbf{F}$.
- Elastic stiffness matrix is $[\mathbf{K}_m] = [\mathbf{J}_m]^T[\mathbf{S}_m][\mathbf{J}_m]$.

- For elastic members, $[\mathbf{S}_m]\delta\mathbf{L} = \delta\mathbf{T}$; Elongation is $\delta\mathbf{L}$ for a load $\delta\mathbf{T}$
- The member stiffness matrix is

$$[\mathbf{S}_m] = \begin{bmatrix} \frac{A_1E_1}{l_1} & 0 & 0 & 0 \\ 0 & \frac{A_2E_2}{l_2} & 0 & 0 \\ 0 & 0 & \frac{A_3E_3}{l_3} & 0 \\ 0 & 0 & 0 & \frac{A_4E_4}{l_4} \end{bmatrix}$$

  where l, A and E are length, cross-sectional area and elastic modulus, respectively.
- External force is related to $\delta\mathbf{T}$ by the Jacobian matrix: $[\mathbf{J}_m]^T\delta\mathbf{T} = \delta\mathbf{F}$
- Hence, $[\mathbf{J}_m]^T[\mathbf{S}_m][\mathbf{J}_m]\delta\mathbf{X} = \delta\mathbf{F}$.
- Elastic stiffness matrix is $[\mathbf{K}_m] = [\mathbf{J}_m]^T[\mathbf{S}_m][\mathbf{J}_m]$.

- For elastic members, $[\mathbf{S}_m]\delta\mathbf{L} = \delta\mathbf{T}$; Elongation is $\delta\mathbf{L}$ for a load $\delta\mathbf{T}$
- The member stiffness matrix is

$$[\mathbf{S}_m] = \begin{bmatrix} \frac{A_1 E_1}{l_1} & 0 & 0 & 0 \\ 0 & \frac{A_2 E_2}{l_2} & 0 & 0 \\ 0 & 0 & \frac{A_3 E_3}{l_3} & 0 \\ 0 & 0 & 0 & \frac{A_4 E_4}{l_4} \end{bmatrix}$$

  where l, A and E are length, cross-sectional area and elastic modulus, respectively.
- External force is related to $\delta\mathbf{T}$ by the Jacobian matrix: $[\mathbf{J}_m]^T\delta\mathbf{T} = \delta\mathbf{F}$
- Hence, $[\mathbf{J}_m]^T[\mathbf{S}_m][\mathbf{J}_m]\delta\mathbf{X} = \delta\mathbf{F}$.
- Elastic stiffness matrix is $[\mathbf{K}_m] = [\mathbf{J}_m]^T[\mathbf{S}_m][\mathbf{J}_m]$.

- For elastic members, $[\mathbf{S}_m]\delta\mathbf{L} = \delta\mathbf{T}$; Elongation is $\delta\mathbf{L}$ for a load $\delta\mathbf{T}$
- The member stiffness matrix is

$$[\mathbf{S}_m] = \begin{bmatrix} \frac{A_1 E_1}{l_1} & 0 & 0 & 0 \\ 0 & \frac{A_2 E_2}{l_2} & 0 & 0 \\ 0 & 0 & \frac{A_3 E_3}{l_3} & 0 \\ 0 & 0 & 0 & \frac{A_4 E_4}{l_4} \end{bmatrix}$$

  where l, A and E are length, cross-sectional area and elastic modulus, respectively.
- External force is related to $\delta\mathbf{T}$ by the Jacobian matrix: $[\mathbf{J}_m]^T\delta\mathbf{T} = \delta\mathbf{F}$
- Hence, $[\mathbf{J}_m]^T[\mathbf{S}_m][\mathbf{J}_m]\delta\mathbf{X} = \delta\mathbf{F}$.
- Elastic stiffness matrix is $[\mathbf{K}_m] = [\mathbf{J}_m]^T[\mathbf{S}_m][\mathbf{J}_m]$.

Static Analysis of SLE based Masts

Links segments – Bending

- For rotations $\delta\phi''$ and member moments $\delta\mathbf{M}''$

$$[\mathbf{S}_n]\delta\phi = \delta\mathbf{M}$$

- The member stiffness matrix $[\mathbf{S_n}]$ for the SLE is given by

$$[\mathbf{S}_n] = \begin{bmatrix} \frac{3E_1 I_z}{l_1+l_2} & 0 & 0 & 0 \\ 0 & \frac{3E_1 I_y}{l_1+l_2} & 0 & 0 \\ 0 & 0 & \frac{3E_2 I_z}{l_3+l_4} & 0 \\ 0 & 0 & 0 & \frac{3E_2 I_y}{l_3+l_4} \end{bmatrix}$$

  E is the Young's modulus, I_z and I_y are moments of inertia.
- Elastic stiffness matrix – $[\mathbf{K}_n] = [\mathbf{J}_n]^T[\mathbf{S}_n][\mathbf{J}_n]$
- Combined stiffness matrix

$$[\mathbf{K}_s] = [\mathbf{K}_m] + [\mathbf{K}_n]$$

Static Analysis of SLE based Masts

Links segments – Bending

- For rotations $\delta\phi''$ and member moments $\delta\mathbf{M}''$

$$[\mathbf{S}_n]\delta\phi = \delta\mathbf{M}$$

- The member stiffness matrix $[\mathbf{S_n}]$ for the SLE is given by

$$[\mathbf{S}_n] = \begin{bmatrix} \frac{3E_1 I_z}{l_1+l_2} & 0 & 0 & 0 \\ 0 & \frac{3E_1 I_y}{l_1+l_2} & 0 & 0 \\ 0 & 0 & \frac{3E_2 I_z}{l_3+l_4} & 0 \\ 0 & 0 & 0 & \frac{3E_2 I_y}{l_3+l_4} \end{bmatrix}$$

  E is the Young's modulus, I_z and I_y are moments of inertia.

- Elastic stiffness matrix – $[\mathbf{K}_n] = [\mathbf{J}_n]^T[\mathbf{S}_n][\mathbf{J}_n]$
- Combined stiffness matrix

$$[\mathbf{K}_s] = [\mathbf{K}_m] + [\mathbf{K}_n]$$

Static Analysis of SLE based Masts

Links segments – Bending

- For rotations $\delta\phi''$ and member moments $\delta\mathbf{M}''$

$$[\mathbf{S}_n]\delta\phi = \delta\mathbf{M}$$

- The member stiffness matrix $[\mathbf{S_n}]$ for the SLE is given by

$$[\mathbf{S}_n] = \begin{bmatrix} \frac{3E_1 I_z}{l_1+l_2} & 0 & 0 & 0 \\ 0 & \frac{3E_1 I_y}{l_1+l_2} & 0 & 0 \\ 0 & 0 & \frac{3E_2 I_z}{l_3+l_4} & 0 \\ 0 & 0 & 0 & \frac{3E_2 I_y}{l_3+l_4} \end{bmatrix}$$

E is the Young's modulus, I_z and I_y are moments of inertia.

- Elastic stiffness matrix – $[\mathbf{K}_n] = [\mathbf{J}_n]^T[\mathbf{S}_n][\mathbf{J}_n]$
- Combined stiffness matrix

$$[\mathrm{K}_s] = [\mathrm{K}_m] + [\mathrm{K}_n]$$

- For rotations $\delta\phi''$ and member moments $\delta\mathbf{M}''$

$$[\mathbf{S}_n]\delta\phi = \delta\mathbf{M}$$

- The member stiffness matrix $[\mathbf{S_n}]$ for the SLE is given by

$$[\mathbf{S}_n] = \begin{bmatrix} \frac{3E_1 I_z}{l_1+l_2} & 0 & 0 & 0 \\ 0 & \frac{3E_1 I_y}{l_1+l_2} & 0 & 0 \\ 0 & 0 & \frac{3E_2 I_z}{l_3+l_4} & 0 \\ 0 & 0 & 0 & \frac{3E_2 I_y}{l_3+l_4} \end{bmatrix}$$

E is the Young's modulus, I_z and I_y are moments of inertia.

- Elastic stiffness matrix – $[\mathbf{K}_n] = [\mathbf{J}_n]^T[\mathbf{S}_n][\mathbf{J}_n]$
- Combined stiffness matrix

$$[\mathbf{K}_s] = [\mathbf{K}_m] + [\mathbf{K}_n]$$

Static Analysis of SLE based Masts

Rank of Stiffness Matrix

- Stiffness matrix is given by $[\mathbf{K}_s] = [\mathbf{J}_s]^T[\mathbf{S}_s][\mathbf{J}_s]$ where

$$[\mathbf{S}_s] = \begin{bmatrix} \frac{A_1E_1}{l_1} & 0 & 0 & 0 & 0 & 0 & 0 & 0 \\ 0 & \frac{A_2E_2}{l_2} & 0 & 0 & 0 & 0 & 0 & 0 \\ 0 & 0 & \frac{A_3E_3}{l_3} & 0 & 0 & 0 & 0 & 0 \\ 0 & 0 & 0 & \frac{A_4E_4}{l_4} & 0 & 0 & 0 & 0 \\ 0 & 0 & 0 & 0 & \frac{3E_1I_z}{l_1+l_2} & 0 & 0 & 0 \\ 0 & 0 & 0 & 0 & 0 & \frac{3E_1I_y}{l_1+l_2} & 0 & 0 \\ 0 & 0 & 0 & 0 & 0 & 0 & \frac{3E_2I_z}{l_3+l_4} & 0 \\ 0 & 0 & 0 & 0 & 0 & 0 & 0 & \frac{3E_2I_y}{l_3+l_4} \end{bmatrix}$$

- Rank of stiffness matrix $[\mathbf{K}_s]$ same as rank of Jacobian matrix

$$rank([\mathbf{K}_s]) = rank(([\mathbf{J}_s][\mathbf{S}_s])^T([\mathbf{J}_s][\mathbf{S}_s])) = rank([\mathbf{J}_s][\mathbf{S}_s]) = rank([\mathbf{J}_s])$$

- Cable modeled as bar capable of taking tension only.

- Stiffness matrix is given by $[\mathbf{K}_s] = [\mathbf{J}_s]^T [\mathbf{S}_s][\mathbf{J}_s]$ where

$$[\mathbf{S}_s] = \begin{bmatrix} \frac{A_1E_1}{l_1} & 0 & 0 & 0 & 0 & 0 & 0 & 0 \\ 0 & \frac{A_2E_2}{l_2} & 0 & 0 & 0 & 0 & 0 & 0 \\ 0 & 0 & \frac{A_3E_3}{l_3} & 0 & 0 & 0 & 0 & 0 \\ 0 & 0 & 0 & \frac{A_4E_4}{l_4} & 0 & 0 & 0 & 0 \\ 0 & 0 & 0 & 0 & \frac{3E_1I_z}{l_1+l_2} & 0 & 0 & 0 \\ 0 & 0 & 0 & 0 & 0 & \frac{3E_1I_y}{l_1+l_2} & 0 & 0 \\ 0 & 0 & 0 & 0 & 0 & 0 & \frac{3E_2I_z}{l_3+l_4} & 0 \\ 0 & 0 & 0 & 0 & 0 & 0 & 0 & \frac{3E_2I_y}{l_3+l_4} \end{bmatrix}$$

- Rank of stiffness matrix $[\mathbf{K}_s]$ same as rank of Jacobian matrix

$$rank([\mathbf{K}_s]) = rank(([\mathbf{J}_s][\mathbf{S}_s])^T([\mathbf{J}_s][\mathbf{S}_s])) = rank([\mathbf{J}_s][\mathbf{S}_s]) = rank([\mathbf{J}_s])$$

- Cable modeled as bar capable of taking tension only.

- Stiffness matrix is given by $[\mathbf{K}_s] = [\mathbf{J}_s]^T[\mathbf{S}_s][\mathbf{J}_s]$ where

$$[\mathbf{S}_s] = \begin{bmatrix} \frac{A_1E_1}{l_1} & 0 & 0 & 0 & 0 & 0 & 0 & 0 \\ 0 & \frac{A_2E_2}{l_2} & 0 & 0 & 0 & 0 & 0 & 0 \\ 0 & 0 & \frac{A_3E_3}{l_3} & 0 & 0 & 0 & 0 & 0 \\ 0 & 0 & 0 & \frac{A_4E_4}{l_4} & 0 & 0 & 0 & 0 \\ 0 & 0 & 0 & 0 & \frac{3E_1I_z}{l_1+l_2} & 0 & 0 & 0 \\ 0 & 0 & 0 & 0 & 0 & \frac{3E_1I_y}{l_1+l_2} & 0 & 0 \\ 0 & 0 & 0 & 0 & 0 & 0 & \frac{3E_2I_z}{l_3+l_4} & 0 \\ 0 & 0 & 0 & 0 & 0 & 0 & 0 & \frac{3E_2I_y}{l_3+l_4} \end{bmatrix}$$

- Rank of stiffness matrix $[\mathbf{K}_s]$ same as rank of Jacobian matrix

$$rank([\mathbf{K}_s]) = rank(([\mathbf{J}_s][\mathbf{S}_s])^T([\mathbf{J}_s][\mathbf{S}_s])) = rank([\mathbf{J}_s][\mathbf{S}_s]) = rank([\mathbf{J}_s])$$

- Cable modeled as bar capable of taking tension only.

Static Analysis of SLE based Masts

Examples

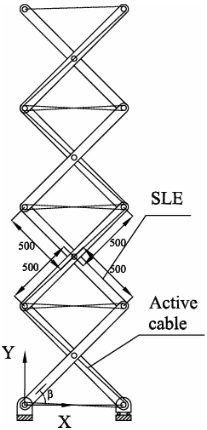

Figure 62: Stacked SLE units

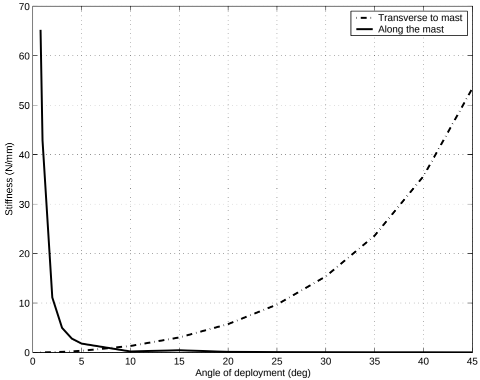

Figure 63: Axial and lateral stiffness during deployment

- Deployment from $\beta = 0$ to $\beta = 45^\circ$, 0.5 N applied along X and Y.
- $AE = 1.5 \times 10^5$ N, $L = 1m$, $EI_z = 9.6 \times 10^7$ Nmm^2.
- Results match with those presented in Kwan and Pellegrino (1994).

Static Analysis of SLE based Masts

Examples

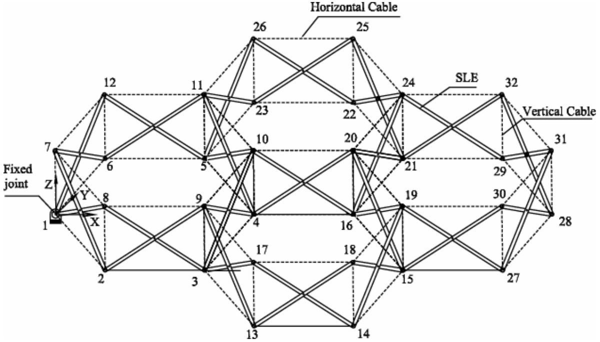

Figure 64: Nested hexagonal SLE mast with cables

	X stiffness (N/mm)	Y stiffness in (N/mm)	Z stiffness (N/mm)
Top or bottom cables	32.01	104.31	17.56
Only vertical cables	40.46	81.17	10.28
Top and bottom cables	65.44	175.42	27.25
All cables	114.23	326.64	39.26

Table 3: Variation of stiffness with addition of cables for assembled hexagonal mast

SUMMARY

- Over-constrained mechanisms and many deployable structures do not give correct DOF using Grübler-Kutzbach criterion.
- Deployable structures are very important for space and other applications.
- A constraint Jacobian based approach is useful to
  - Determine correct DOF of over-constrained mechanisms and deployable structures.
  - Determine redundant links and joints which make such mechanisms violate Grübler-Kutzbach criterion.
- Kinematic and static analysis of several pantograph based structures performed.

SUMMARY

- Over-constrained mechanisms and many deployable structures do not give correct DOF using Grübler-Kutzbach criterion.
- Deployable structures are very important for space and other applications.
- A constraint Jacobian based approach is useful to
  - Determine correct DOF of over-constrained mechanisms and deployable structures.
  - Determine redundant links and joints which make such mechanisms violate Grübler-Kutzbach criterion.
- Kinematic and static analysis of several pantograph based structures performed.

SUMMARY

- Over-constrained mechanisms and many deployable structures do not give correct DOF using Grübler-Kutzbach criterion.
- Deployable structures are very important for space and other applications.
- A constraint Jacobian based approach is useful to
  - Determine correct DOF of over-constrained mechanisms and deployable structures.
  - Determine redundant links and joints which make such mechanisms violate Grübler-Kutzbach criterion.
- Kinematic and static analysis of several pantograph based structures performed.

SUMMARY

- Over-constrained mechanisms and many deployable structures do not give correct DOF using Grübler-Kutzbach criterion.
- Deployable structures are very important for space and other applications.
- A constraint Jacobian based approach is useful to
  - Determine correct DOF of over-constrained mechanisms and deployable structures.
  - Determine redundant links and joints which make such mechanisms violate Grübler-Kutzbach criterion.
- Kinematic and static analysis of several pantograph based structures performed.

OUTLINE

- References & Sugested Reading